



# Seasonal and Interannual Drivers of Sargassum Inundations in the Northern Gulf of Guinea

Clovis Thouvenin-Masson<sup>1</sup>, Julien Jouanno<sup>1</sup>

<sup>1</sup>IRD, LEGOS, Toulouse, France

5 *Correspondence to:* Clovis Thouvenin-Masson (clovis.thouvenin-masson@univ-tlse3.fr)

**Abstract:** Sargassum strandings have become recurrent along the northern Gulf of Guinea (n-GoG) and are reported in the literature as having significant societal impacts, particularly on fisheries. However, persistent cloud cover frequently hampers satellite detection in this region, complicating efforts to monitor and study the phenomenon. To overcome this limitation, we combine remote-sensing observations with process-oriented numerical simulations that represent Sargassum transport, growth, and stranding. This approach provides new insights into the seasonal cycle and the interannual variability of coastal arrivals since 2011. Both observations and the model reveal a semiannual cycle of arrivals along the n-GoG, with peaks in March-April-May and September-October-November. Our results suggest that arrivals in the n-GoG depend primarily on the advection of Sargassum from the eastern Tropical Atlantic (e-TA), whereas local growth appears to play only a minor role. Indeed, a prior build-up of biomass preconditions n-GoG Sargassum intrusion events: off Sierra Leone for spring events, and within the ITCZ for autumn events. In both seasons, transport toward West Africa occurs via the North Equatorial Counter Current (NECC) and the Guinea Current (GC), and is particularly strong in autumn, with an advection time of about three months between the e-TA and the n-GoG coasts. After crossing Cape Palmas, Sargassum is driven shoreward by the prevailing southerly winds, which both promote coastal accumulation and maintain Sargassum north of the Equator. Without this wind-driven transport, Sargassum would remain embedded in the GC, spread more broadly across the Gulf of Guinea (GoG), and could recirculate southward through the South Equatorial Current (SEC). Coastal stranding acts as an additional regulator of the regional distribution by removing biomass from the open ocean and limiting its persistence near the coast. At interannual timescales, variability is controlled first by the amount of Sargassum biomass in the e-TA and second by their latitudinal position and likelihood of crossing Cape Palmas, especially in autumn. Both factors appear to be linked to the Atlantic Meridional Mode (AMM), with negative phases favoring entry into the GoG.

## 25 1 Introduction

Pelagic Sargassum has become a major oceanographic and societal issue in the tropical Atlantic over the last decade. Since 2011, large strandings have been reported in the Caribbean (Franks et al., 2012; León-Pérez, et al., 2021), along the Brazilian coast (Amorim et al., 2025a; Sissini et al., 2017), and on West African shores (Sowah et al., 2022a). The floating species involved are *Sargassum natans* and *Sargassum fluitans*, long known from the Sargasso Sea (Carpenter and Cox, 1974;



30 Niermann, 1986). Since 2011, persistent populations have also proliferated in the tropical belt, forming the “Great Atlantic Sargassum Belt” (GASB), which extends from West Africa to the Caribbean and Gulf of Mexico (Wang et al., 2019). The GASB is widely regarded as the main source of the exceptional mass strandings observed since 2011 on Caribbean coasts.

Stranding events are now frequent and widespread and are considered a new natural hazard for tropical Atlantic coasts (e.g., Bernard et al., 2021; Jouanno et al., 2025b). Although floating Sargassum provides habitat and nursery grounds for many  
35 species (Witherington et al., 2012), its impacts at the coast are largely negative. Accumulated biomass depletes oxygen levels, degrades water quality, and harms seagrasses and corals (van Tussenbroek et al., 2017), while stranded Sargassum releases hydrogen sulfide and ammonia. In Mexico in 2018, more than 70 species died and water quality deterioration extended hundreds of meters offshore (Rodríguez-Martínez et al., 2019). At the same time, interest is growing in the use of this biomass for fertilizer, animal feed, biofuels, construction blocks, and bioplastics, although variable supply, logistical constraints, and  
40 compositional variability remain major challenges (Chávez et al., 2020; López Miranda et al., 2021; Maneein et al., 2021; Milledge and Harvey, 2016; Azcorra-May et al., 2022; Robledo et al., 2021; Thompson et al., 2020).

In West Africa, stranded biomass is thought to be lower than in the Caribbean (Jouanno et al., 2025b), but the quantities washed ashore are still substantial and cause significant nuisance. A recent regional review further documents the ecological, socio-economic and health impacts of these events, and highlights the limited adaptive capacity and fragmented management  
45 responses across West Africa (Saba et al., 2025). Reported impacts include foul odors, clogged fishing nets, reduced fish catches, and engine failures. In this region, tourism and small-scale fisheries are especially vulnerable, and cleanup costs are high for governments (Yaw Atiglo et al., 2024).

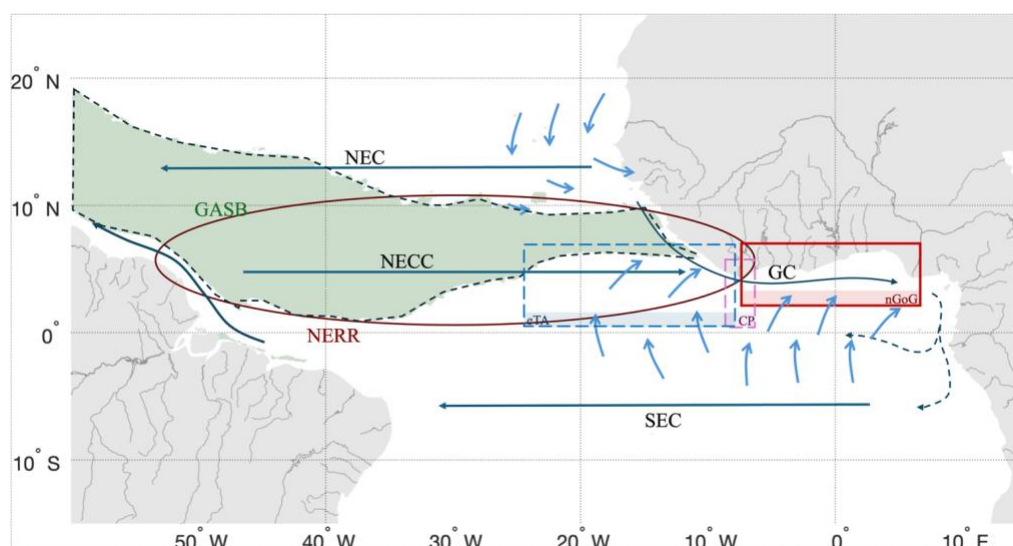
The emergence of the North Equatorial Recirculation Region (NERR; Figure 1) as a key reservoir of the seasonal Sargassum proliferation has been documented by satellite since 2011 (Gower et al., 2013) and is now considered a central component of  
50 the GASB system (Johns et al., 2020; Jouanno et al., 2021, 2025a; Wang et al., 2019). Although the drivers of the post-2011 proliferation remain debated, there is evidence that circulation anomalies associated with the extreme 2009-2010 NAO may have advected Sargassum southward from the Sargasso Sea to the Tropical Atlantic where it encountered conditions favorable to its proliferation and maintenance for more than 15 years (Johns et al., 2020; Jouanno et al., 2025a). Once aggregated along the ITCZ in the tropical Atlantic, Sargassum is transported mainly by currents and wind drift toward the Caribbean (Putman  
55 et al., 2018, 2020; Brooks et al., 2018). However, recurrent arrivals have also been observed in the Gulf of Guinea (Fidai et al., 2025), which suggests that some of this Atlantic biomass ultimately reaches West African coasts.

Despite growing impacts, research in the Eastern Tropical Atlantic remains sparse compared to the Caribbean: only about 3.5 % of Sargassum studies published since 2010 focus on West Africa (Yaw Atiglo et al., 2024). Nevertheless, the studies conducted so far allow us to map the extent of the affected coastline (Figure 2) Chemical and morphological analyses of  
60 beached biomass in Ghana and Nigeria have confirmed the presence of mixed populations of *S. natans* and *S. fluitans* (Addico and deGraft-Johnson, 2016; Oyesiku and Egunyomi, 2014). Surveys in Nigeria indicated that arrivals coincided with the rainy



season (May-August), suggesting a link with monsoon dynamics (Solarin et al., 2014). Satellite-based detection along the coast from Sierra Leone to Nigeria between 2011 and 2016 confirmed the recurrence of nearshore aggregations, although cloud cover associated with the ITCZ hampered the analysis (Adet et al., 2017). Reported influx severity varies regionally: Ghana, Nigeria and Ivory Coast are most frequently described as heavily impacted, whereas Benin is rarely documented (only DGEC and MCVDD, 2020). A recent synthesis by Fidai et al. (2025) provided the first systematic attempt to characterize seasonal and interannual variability of Sargassum influxes in the e-TA, including the GoG. Their results revealed peaks in September and in March-May, demonstrating that the regional seasonality differs from the well-established boreal spring-summer peak observed in the Caribbean. They also highlighted contrasting views on transport pathways: some authors argue for input from the Amazon plume and western sources, whereas others suggest export from the GoG itself toward the tropical Atlantic (Brooks et al., 2018; Fidai et al., 2025; Franks et al., 2016; Gobert et al., 2025). These findings underscore that, although Sargassum has become a regular feature of West African coasts, its seasonal cycle, variability, and drivers remain poorly understood compared with those of the western basin.

In this study, we investigate when and why Sargassum reaches the northern n-GoG by documenting its seasonal climatology and interannual variability since 2011, and by identifying the physical and biogeochemical conditions that produce unusually strong Sargassum stranding events. We use  $1/12^\circ$  NEMO-Sarg simulations (Jouanno et al., 2021) of the equatorial and north Atlantic to represent transport, growth and stranding dynamics of the Sargassum and complement them with Lagrangian trajectory analysis using PARCELS software (Delandmeter and Van Sebille, 2019a) to characterize typical pathways and the sources of extreme arrivals. This combined framework provides a coherent picture of Sargassum dynamics in the n-GoG.



80

Figure 1: Schematic of circulation, source regions, and analysis boxes. The Great Atlantic Sargassum Belt (GASB, green shading), the North Equatorial Recirculation Region (NERR, red contour) and principal currents — North Equatorial Current (NEC), North Equatorial Countercurrent (NECC), Guinea Current (GC), South Equatorial Current (SEC) — are shown. Boxes denote e-TA (blue dashed), Cape Palmas gate (purple dashed), and the n-GoG analysis region (red). Arrows sketch typical wind forcings.



## 85      2    **Methods**

### **2.1 Remote-sensing detection of Sargassum cover**

Pelagic Sargassum cover were derived from ocean-color sensors, primarily MODIS aboard NASA *Aqua* (since mid-2002) and *Terra* (since 2000) satellites, and processed by Descloitres et al. (2021). Weekly and monthly averages of fractional coverage were computed by averaging daily values on a  $1/4^\circ$  grid, while the number of valid daily observations was retained as an indicator of sampling reliability. A well-known limitation of optical satellite detection is its strong sensitivity to cloud cover and sun glint, both of which frequently obscure the ocean surface in the tropics and reduce the number of valid retrievals (Podlejski et al., 2022; Wang and Hu, 2016). This limitation is particularly severe during the boreal summer rainy season in the GoG, when persistent cloudiness affects much of the region. In addition, nearshore areas are often excluded during processing because of adjacency effects and mixed signals from land, shallow waters, and suspended sediments, which can generate false positives if not properly masked (Wang and Hu, 2016).

### **2.2 Simulations of Sargassum dynamics**

To account for the transport and growth-decay properties of Sargassum, we rely on the NEMO-Sarg1.0 model (Jouanno et al., 2021). This model explicitly couples the transport of pelagic *Sargassum* with a physiological module representing growth, nutrient uptake, and mortality. It is embedded within the NEMO ocean-circulation framework. NEMO-Sarg has already been applied and validated in several contexts. In particular, it has demonstrated its ability to reproduce the emergence of the GASB (Jouanno et al., 2025a) and seasonal forecast experiments have shown predictive skill at lead time of up to seven months (Jouanno et al., 2023). However, because the model does not fully reproduce the observed interannual variations in biomass over recent years, as discussed in Jouanno et al. (2025a), we use here a version nudged towards 7-day averages of Sargassum fractional cover derived from MODIS observations (see Sect. 2.1) following the approach described in Jouanno et al. (2025b). Nudging is applied west of  $15^\circ\text{W}$ , leaving the e-TA and the GoG free to evolve dynamically and biologically. This strategy allows the model to realistically represent the seasonal and interannual supply of Sargassum to the e-TA and GoG. Transport is represented as the sum of surface currents from GLORYS12, Stokes drift, and a windage contribution equal to 0.1% of the 10 m wind speed, derived from the ERA5 reanalysis. Table 1 summarizes the main forcings, their origin, and their use in this study.

110



Table 1: Summary of the forcings used in the SARG12 simulation and in this study. The forcings used in the sensitivity experiments are described below.

Variables	Source	Temporal resolution	Reference paper
Ocean currents, temperature, salinity	GLORYS 1/12°	Daily	(Lellouche et al., 2021)
Nutrients (NO <sub>3</sub> , PO <sub>4</sub> , NH <sub>4</sub> , Fe)	NEMO-PISCES ¼°	Monthly	(Berthet et al., 2019)
Solar radiation, 10 m winds, stokes drift	ERA5	Daily	(Hersbach et al., 2020)

115

Sensitivity experiments were designed to identify the main sources of variability in Sargassum dynamics in the n-GoG. The reference simulation (SARG12) is compared with two sensitivity experiments in which a single process is modified. All simulations use identical ocean physics, biogeochemistry, atmospheric forcing, and model domain relative to the reference configuration. In SARG12-nostranding, coastal biomass loss due to stranding is suppressed, allowing assessment of the role of stranding in shaping the simulated Sargassum distribution within the GoG. In SARG12-nowind, both Stokes drift and windage are excluded, isolating the contribution of wind-driven processes to Sargassum transport. A summary of the experiments is provided in Table 2.

120

Table 2: List of model experiments and differences between them.

Experiment	Purpose	Nudging (west of 15° W)	Windage+Stokes	Stranding
SARG12	Baseline simulation, with realistic year-to-year supply and full physics	Interannual monthly MODIS observations	ON	ON
SARG12-nostranding	Quantify the role of beaching losses	Same as SARG12	ON	OFF
SARG12-nowind	Quantify the role of direct wind forcing on transport	Same as SARG12	OFF	ON

125



### 2.3 Study domains

To diagnose how remote Sargassum stocks may contribute to coastal arrivals, we defined fixed geographic boxes, shown in Figure 1. The n-GoG is our target region, where we compute a monthly mean Sargassum cover index. Two additional regions are used to characterize potential upstream pathways feeding the coast: a box around Cape Palmas and a broader eastern tropical Atlantic box (“e-TA”) that samples the NECC/GC corridor.

Within each box, we analyze candidate drivers of n-GoG arrivals, including physical variables such as currents, winds, sea surface temperature and salinity, chlorophyll, and the Sargassum fractional cover itself. To relate upstream signals to downstream coastal peaks, simple time offsets are applied between boxes; these lags are defined in sect. 3.2.

Table 3: Definition of the boxes shown in Figure 1

Region (name)	Longitude (°E)	Latitude (°N)	Purpose / metric
Northern Gulf of Guinea Coast (n-GoG)	[-7.5 7]	[2 7]	Target signal: coastal mean Sargassum fractional coverage
Cape Palmas	[-8.5 -7.5]	[2 7]	Gateway: Sargassum crossing near the cape
Eastern tropical Atlantic (e-TA)	[-25 -7.5]	[0 7]	Equatorial stock: NECC/GC source region

### 2.4 Backward Lagrangian experiments

The transport pathways of floating Sargassum reaching the n-GoG are investigated using the Lagrangian framework Parcels (Amorim et al., 2025b; Delandmeter and Van Sebille, 2019b). Particles were integrated backward in time from locations where Sargassum was present in the model. For each simulation year, particles were seeded at mid-month in April and October, corresponding to two representative seasons of Sargassum occurrence in the n-GoG. Seeding was performed at all surface grid points within the n-GoG where the simulated Sargassum fractional coverage exceeded  $2 \times 10^{-5}$ , ensuring that particles originated only from locations where Sargassum biomass was present in the model. Particles were then advected backward for 120 days using GLORYS surface currents. A windage contribution equal to 1 % of the 10 m wind velocity was included to represent the combined effect of windage and Stokes drift on floating Sargassum. Particle trajectories were integrated using a fourth-order Runge–Kutta scheme with a 6-hour time step. To diagnose the dominant pathways, all trajectory positions were accumulated in  $0.1^\circ \times 0.1^\circ$  spatial bins. For each grid cell, we computed both (i) the mean advection time required for particles to reach that location and (ii) the fraction of trajectory occurrences, defined as the number of trajectory points passing through



the cell normalized by the total number of trajectory points. These diagnostics provide complementary information on the  
150 characteristic transport timescales and the preferred transport corridors linking the tropical Atlantic to the n-GoG.

## 2.5 Forward Lagrangian experiments

To further assess the role of wind forcing in shaping Sargassum pathways from the e-TA toward the GoG, we performed a set  
of idealized forward Lagrangian experiments using the same Parcels framework and numerical settings as in Sect. 2.4. In  
contrast to the backward experiments, particles were seeded in the source region and integrated forward in time in order to  
155 quantify their subsequent dispersion and their potential to reach the GoG under different forcing assumptions.

For each month from January 2010 to December 2023, particles were released at mid-month in the e-TA. Seeding was restricted  
to surface grid cells where the simulated Sargassum fractional coverage exceeded  $2 \times 10^{-5}$ , so that particles were released only  
from locations where Sargassum was present in the model. Particles were then advected forward for 360 days. Two  
configurations were considered: a no-wind experiment, using GLORYS surface currents only, and a wind-forced experiment,  
160 using effective surface currents including the wind-driven contribution equivalent to 1 % of the 10 m wind velocity, consistent  
with the parameterization adopted in Sect. 2.4 to represent the combined effects of windage and Stokes drift.

## 3 Results

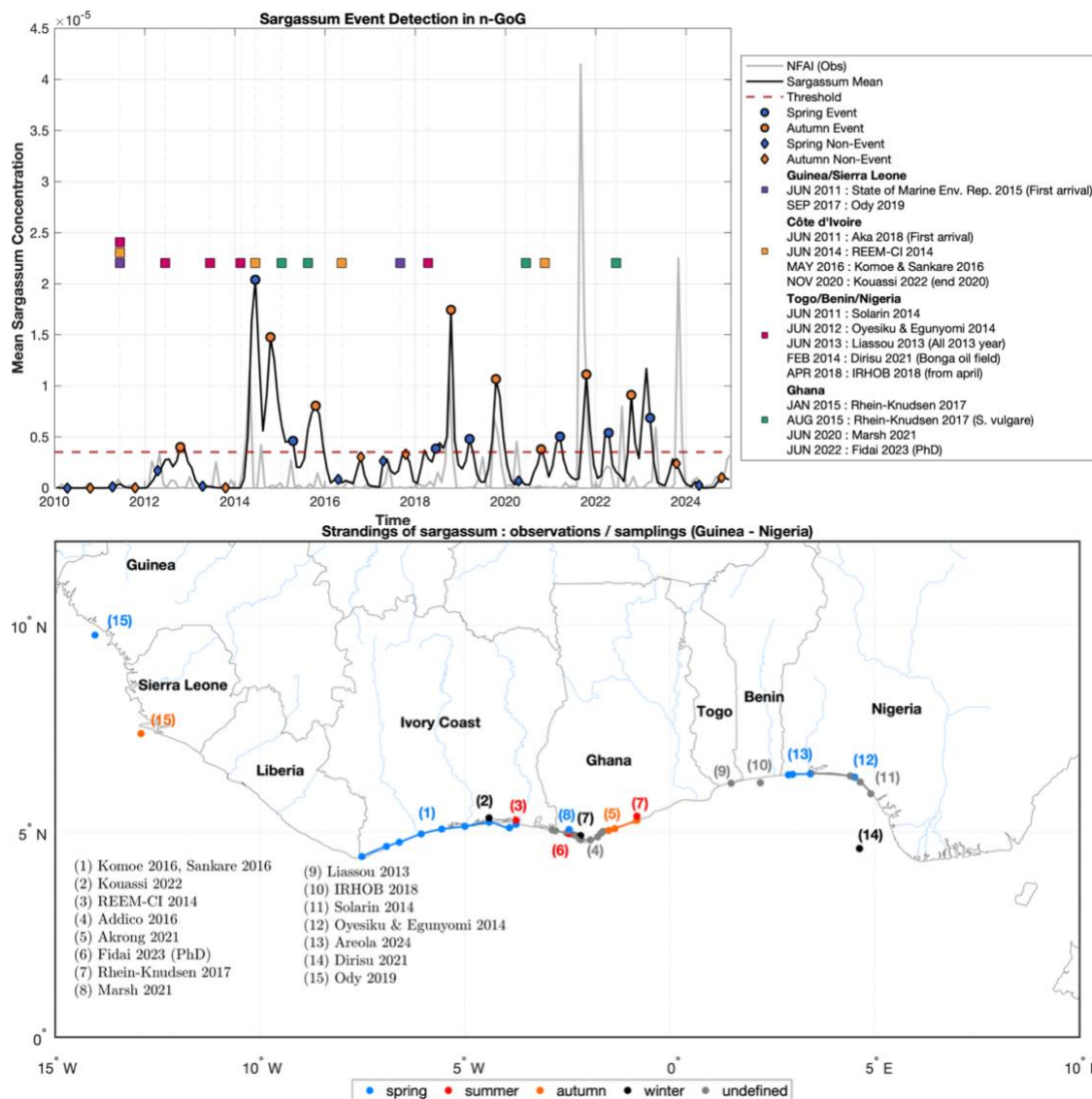
### 3.1 Comparison of the model with observations and previous reports

Several studies have documented Sargassum arrivals along the n-GoG coast since 2011, with recurrent spring and/or autumn  
165 peaks (Figure 2, bottom). For the Guinea-Sierra Leone sector, national and UNEP syntheses report first detections in 2011 and  
typical occurrences from June-October, and later emphasize the 2017 season highlighted by regional surveys (Environment  
Protection Agency, 2015; Ody et al., 2019). In Ivory Coast, coastal monitoring recorded strandings at Grand-Bassam in June  
2014 (REEM-CI, 2021) and widespread landfalls from Grand-Bassam to Tabou in May-June 2016 (Komoe et al., 2016), while  
academic studies place the climatological peak in May and identify 2011 as the year of the first national observations (Aka et  
170 al., 2018).

Farther east, site-specific strandings in Ghana, notably at Egyambra and Mumford, were reported from January to August 2015  
by Addico and deGraft-Johnson (2016), and were later complemented by surveys conducted between 2017 and 2019 at  
Mumford, Komenda and Elmina, partly focused on *Sargassum vulgare* (Akrong et al., 2021). Additional studies report major  
inputs in 2011-2012 (Ackah-Baidoo, 2013; Fidai et al., 2020), as well as a spring event in 2020 (Marsh et al., 2021). Satellite  
175 and drifter analyses also identified groundings events near Ghana in March 2011-2012 (Johns et al., 2020). For Togo and  
Benin, available sources indicate year-round presence in 2013 (Issifou et al., 2014) and arrivals beginning in April in Benin  
(DGEC and MCVDD, 2020). In Nigeria, studies document spring-summer strandings in 2012 (April-July) in Ondo State  
(Oyesiku and Egunyomi, 2014), and a prolonged sequence from May 2011 to August 2012 along Lagos-Ogun coast (Solarin



et al., 2014). Interviews conducted at Badagry, Gberefu and Ajido suggest that the main events occur in autumn (Areola et al., 2024), while an offshore occurrence near the Bonga field was reported in February 2014 (Dirisu et al., 2021); Overall, most sources describe a main Sargassum season extending from March to October, with occasional persistence into November-December.



185 Figure 2: Temporal and spatial distribution of coastal Sargassum in the Northern Gulf of Guinea (N-GoG), 2010–2024. Top) Time series of coastal Sargassum fractional coverage. The black line shows daily model-based mean coverage, while the grey line represents satellite observations. The dashed red line indicates the percentile-based event threshold. Blue circles mark detected spring Sargassum events. Bottom) Map of documented Sargassum strandings along the N-GoG coastline, from Liberia to Nigeria. Points are color-coded by season of occurrence: blue (spring), yellow (summer), red (autumn), black (winter), and grey (undated). Numbers correspond to references in the bibliography (right).

190

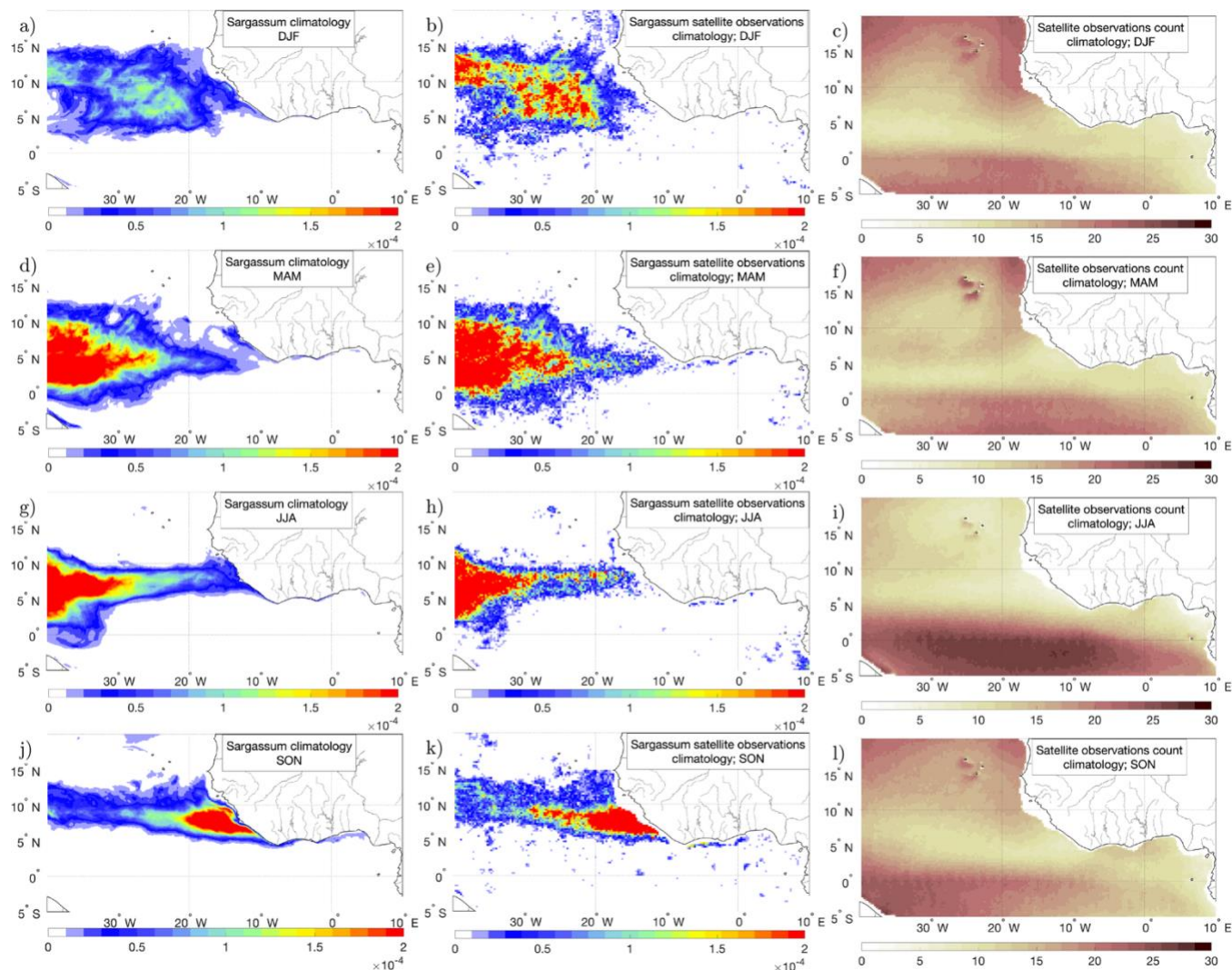


195 Satellite observations are consistent with this seasonality and regional distribution (Figure 3b,e,h,k), with Sargassum arrivals detected mainly in spring and autumn, particularly along the coasts of Ivory Coast and Ghana. In some years, Sargassum is also observed during summer, likely reflecting biomass that persisted from the spring season rather than newly formed arrivals. The remote sensing detections also show recurrent signals farther south, off the coast of the Congo (see, for example, Figure 3h), which, to our knowledge, are not supported by in situ reports and are therefore likely to correspond to false detections. In addition, two very strong coastal peaks in the satellite record, in September 2021 and November 2023 (Figure 2,top, gray line) appear anomalously large and may be overestimated, as no corresponding extreme events have been reported in the literature for these dates.

200 Compared with satellite observations, the reference SARG12 simulation reproduces the main seasonal and interannual occurrences of coastal Sargassum strandings in the n-GoG between 2010 and 2024 reasonably well (Figure 2, top). In particular, the model captures the major spring events reported in 2012, 2014, 2015, 2017, and 2022, with realistic timing and amplitude relative to satellite-derived fractional coverage estimates (Figure 2, top, gray line). Several autumn strandings are also reproduced, including those of 2014, 2018, 2021, and 2023, although their intensity is sometimes overestimated (2014, 2018) or underestimated (2021, 2023). Notably, the model fails to reproduce the spring 2020 peak, which is documented in 205 observations and reported in the literature (Marsh et al., 2021). The model also shows a mismatch from late 2022 to early 2023, when simulated peaks occur earlier than those inferred from satellite data. Both datasets indicate the highest coastal concentrations during boreal autumn along the n-GoG coasts, in agreement with reports of strandings in the literature (Akrong et al., 2021; Fidai et al., 2023; Oyesiku and Egunyomi, 2014; Solarin et al., 2014).

210 Direct comparison between the model and reported coastal strandings remains limited, because relatively few events are documented in the literature, especially in recent years. In addition, satellite detection is affected by cloud cover and land contamination, resulting in patchy observational coverage (Figure 3, right column). These limitations call for caution when interpreting discrepancies between the model and the observations. Nevertheless, the overall agreement in seasonality and spatial distribution provides confidence in the ability of NEMO-Sarg to reproduce the main patterns of Sargassum transport and arrival in the GoG.

215



220

Figure 3: Left: modeled Sargassum FC from SARG12. Middle: satellite Sargassum FC from MODIS. Right: mean number of valid satellite observations per month. From top to bottom: boreal winter (DJF), spring (MAM), summer (JJA), autumn (SON). Note the data sparsity along the n-GoG coast, with <15 valid observations per month on average, which limits direct satellite-based assessment in this region. The period 2010 to 2024 is considered for both model and observations.

225 **3.2 Origins of the Sargassum reaching the n-GoG: Lagrangian advection**

The seasonal distribution shown in Figure 3 suggests that Sargassum observed along the coast of the GoG originate from the e-TA. To test this hypothesis and estimate the transport timescales of the Sargassum reaching the n-GoG during the two main inundation seasons (April and October), we performed backward Lagrangian experiments. Particles were seeded in areas where Sargassum was observed in the e-TA region (see Table 3 for description of the regions). The mean advection time (in days) required for particles released along the n-GoG coast to reach upstream locations along the backtracked trajectories are shown

230



in Figure 4a,c, while the density of trajectory points, expressed as the fraction of total trajectory occurrences in each grid cell and highlighting the preferred transport pathways, is shown in Figure 4b,d.

In both seasons, the backtracking experiments reveal a dominant west-to-east transport pathway linking the e-TA to the n-GoG through the NECC and GC corridor. The trajectory-density maps show that most particles originate from offshore regions of the e-TA and is transported toward the coast over timescales of about two to three months. This lag provides a physical basis for the time offsets used in the subsequent interannual-variability analysis (Section 3.5).

Seasonal differences nevertheless emerge in the spatial structure of the dominant pathways. For particles reaching the coast of the n-GoG in April trajectories are more broadly distributed across the eastern tropical Atlantic (Figure 4b), suggesting that multiple upstream regions may contribute to the coastal Sargassum signal. By contrast, for particles reaching the n-GoG coast in October, trajectory density is more concentrated along a narrower corridor extending from 8° N and following the West African coasts.

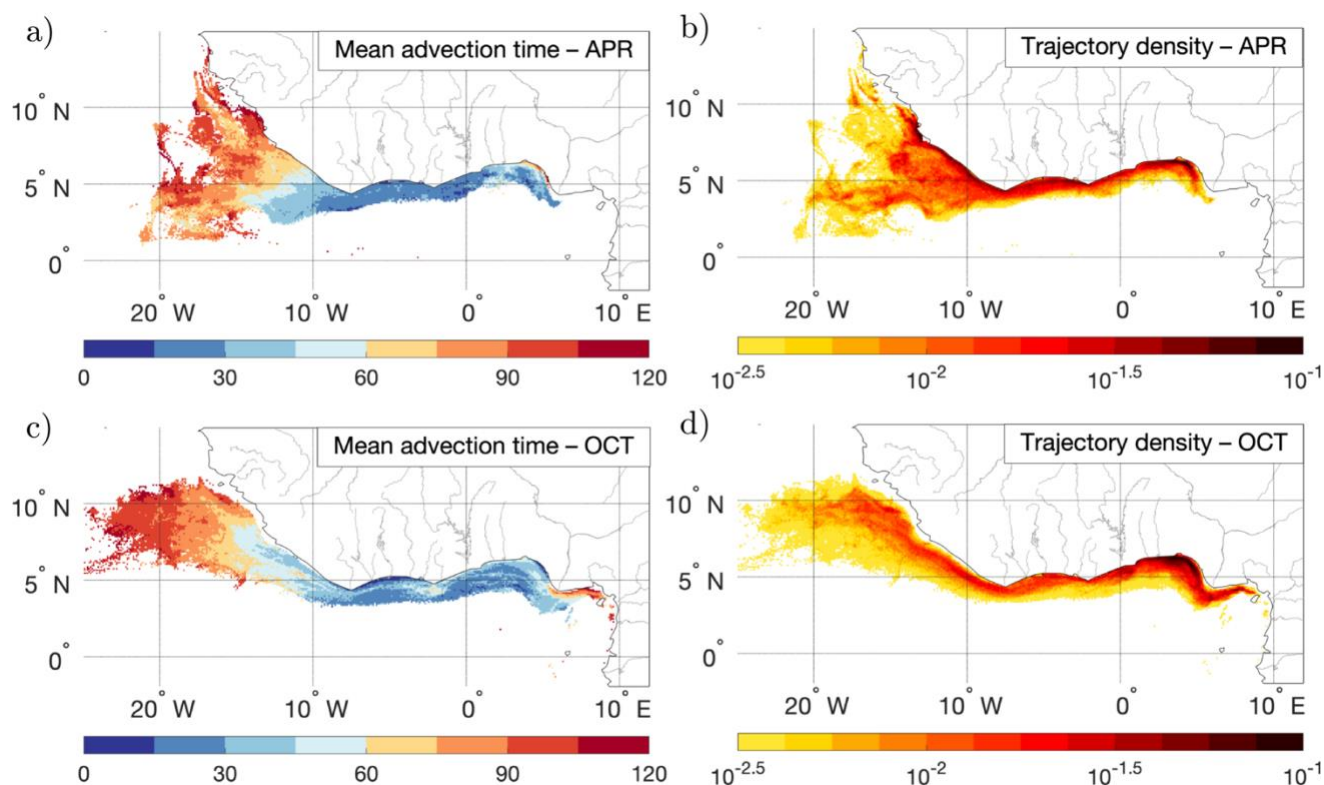


Figure 4: Backtracking diagnostics of coastal Sargassum in the n-GoG derived from Lagrangian simulations. Panels show results aggregated over all available years for two representative months: April (a–b) and October (c–d). Mean advection time (days) from coastal release locations to the upstream positions of the backtracked trajectories are shown in (a,c). Colors indicate the average travel time required for floating Sargassum to reach each  $0.1^\circ \times 0.1^\circ$  grid cell. Relative density of trajectory points per grid cell (b,d) is expressed as a fraction of the total number of trajectory points. This metric highlights the spatial distribution and preferential pathways of the backtracked trajectories. Higher values reveal the dominant transport corridors linking the e-TA to the n-GoG.



250

### 3.3 Seasonality of Sargassum arrivals in the northern Gulf of Guinea

Since 2011, the seasonal cycle of Sargassum influxes in the n-GoG has followed a persistent pattern (Figure 2): a first peak occurs in boreal spring (MAM), followed by a summer lull and then by a second peak in autumn (SON). The Lagrangian diagnostics presented in Section 3.2 indicate that transport from offshore regions of the e-TA to the n-GoG typically occurs over timescales of about two to three months, implying that coastal arrivals reflect oceanic conditions that developed several weeks to months upstream. We now examine the climatological factors underlying this seasonal pattern in each season (Figure 5).

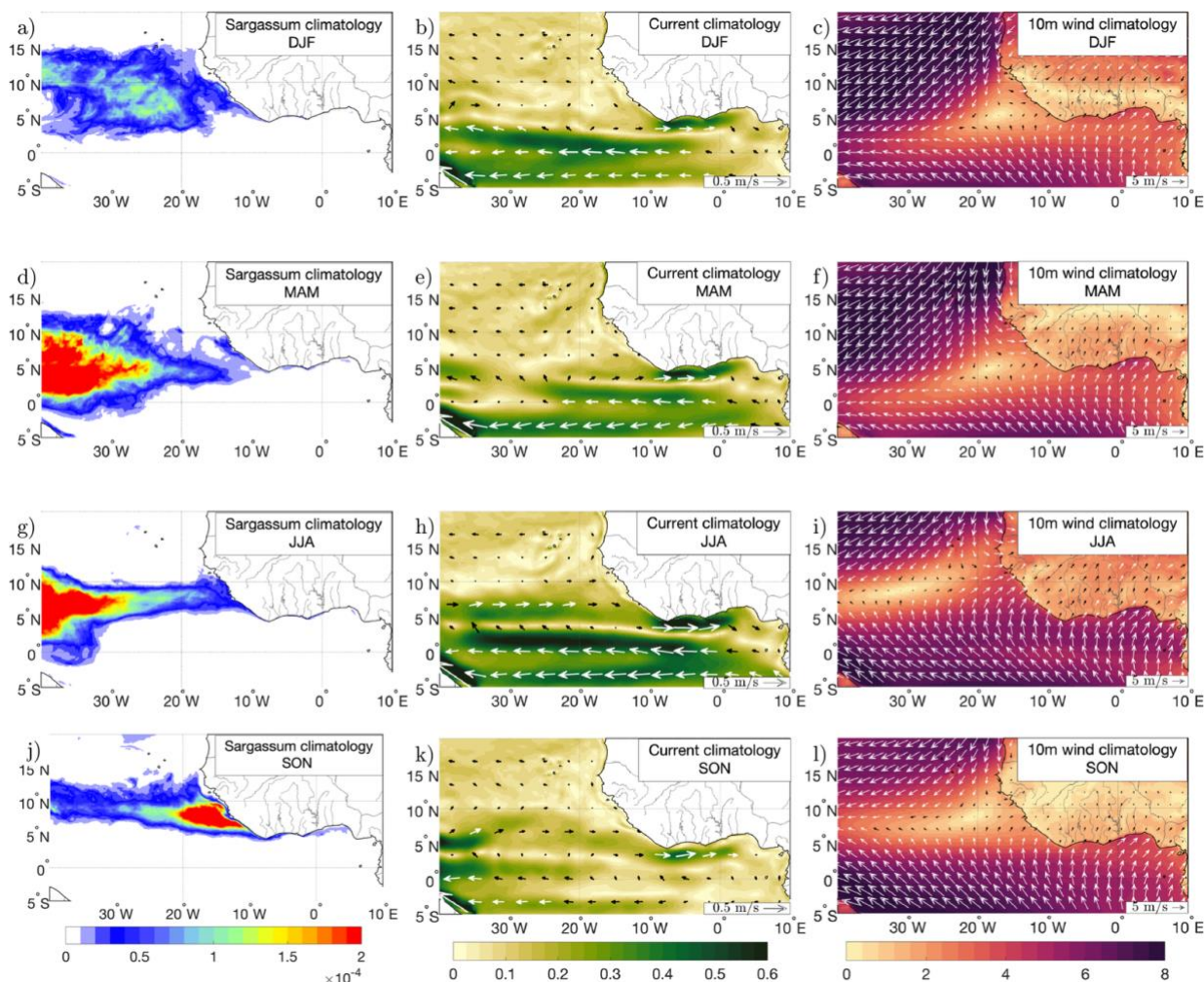
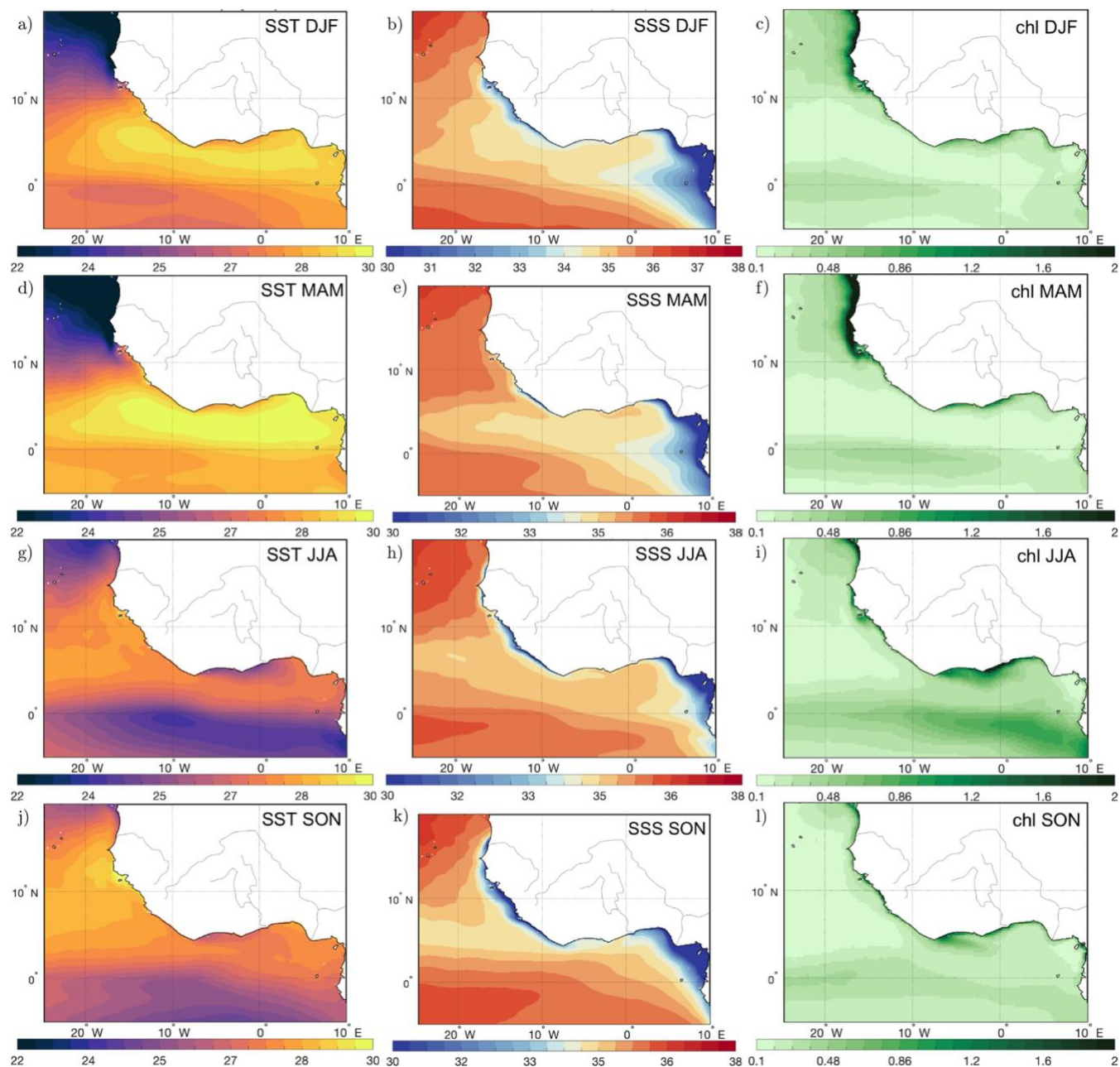


Figure 5: Climatological Sargassum distribution and environmental conditions. (left) Mean Sargassum Fractional Coverage. (center) Surface currents ( $\text{m s}^{-1}$ ). (right) 10 m winds (vectors) over wind speed ( $\text{m s}^{-1}$ ). From top to bottom: DJF, MAM, JJA, and SON seasons.

260



During boreal winter and early spring, the ITCZ is located close to the equator and begins to migrate northward, while the West African monsoon and trade winds remain weak (e.g., Grodsky and Carton, 2003). The NECC is developing and can be intermittent; in its western part it may even reverse westward (Johns et al., 2020). Near Sierra Leone, the GC is present but  
265 weak and flows southeastward; the NECC and GC converge near Cape Palmas, while winds are directed toward the coast (Figure 5b,c). Spring arrivals of Sargassum in the GoG reflect conditions established during late winter and mainly originate from two sources (Figure 5a). First, a residual pool inherited from the previous winter, often trapped off Guinea and Sierra Leone during winter, is advected by the GC. This pathway is partly weakened by southwesterly winds, which push Sargassum toward the coast and oppose southeastward advection along the Sierra Leone - Liberia coast (Figure 5c). A fraction of this  
270 winter stock is also carried westward, seeding the NERR toward Brazil. Second, because the ITCZ lies farther south in spring, Sargassum tends to accumulate near the equator within the convergence zone. Sargassum located sufficiently far south may enter the eastward-flowing NECC and cross Cape Palmas, although transport efficiency remains limited.



275 Figure 6: Seasonal climatologies of the physical surface environment in the eastern tropical Atlantic and Gulf of Guinea, averaged over all years of the analysis period. From left to right: sea surface temperature (SST), sea surface salinity (SSS), and chlorophyll (chl). From top to bottom: boreal winter (DJF), spring (MAM), summer (JJA), and autumn (SON).

Within the GoG during MAM, weak wind forcing leads to minimal coastal upwelling: SST therefore remain high (~28 °C; Figure 6d) and nutrient-rich subsurface waters are not supplied to the surface (Figure A1; Hardman-Mountford and McGlade,

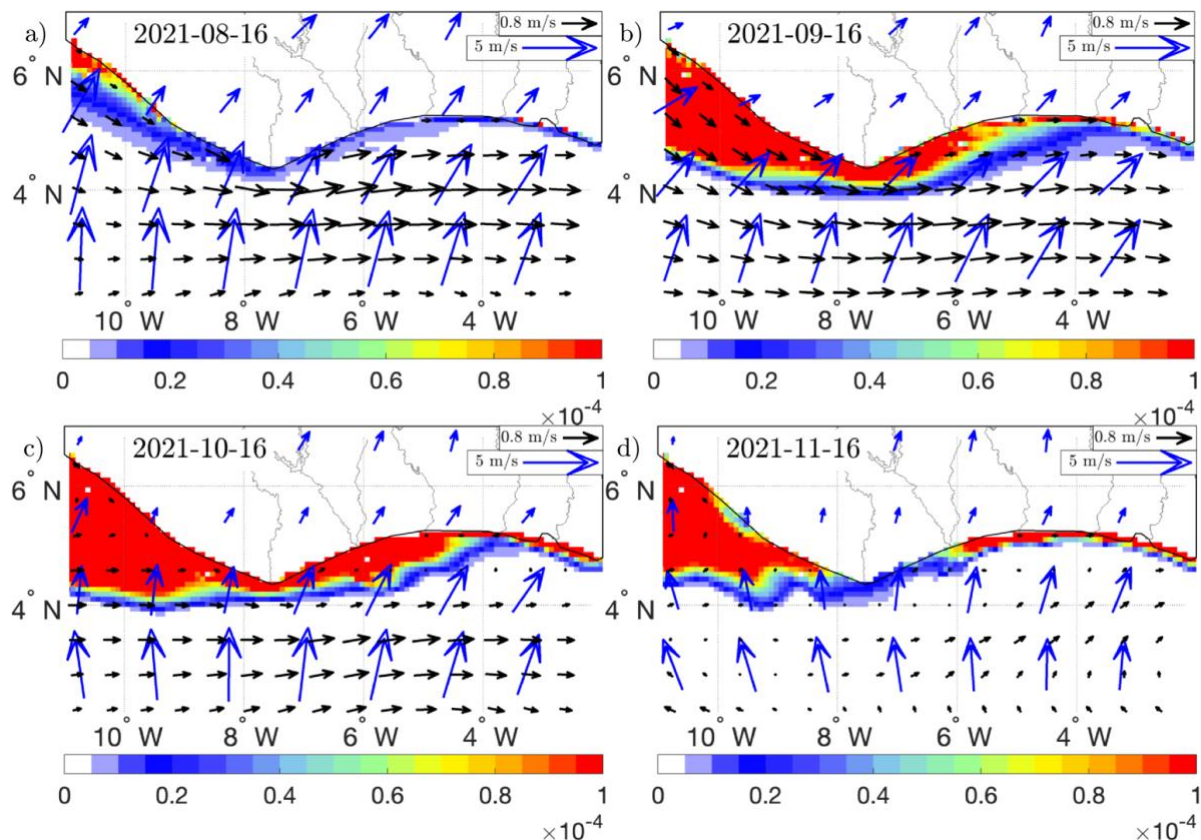


280 2002). Chlorophyll-a remains low (Figure 6f), and growth is reduced in these nutrient-poor conditions. At the same time, southerly winds (Figure 5c), through windage and Stokes drift, tend to push Sargassum northward against the coastline, favoring nearshore accumulation and stranding while limiting export deeper into the Gulf.

In summer, the West African monsoon winds reach their maximum. This drives the seasonal coastal upwelling off Ivory Coast and Ghana and produces cooler SSTs (~25–26 °C, Figure 6g; e.g., Binet, 1997;Djakouré et al., 2024). Rainfall and major river  
285 discharges (e.g., Niger, Volta) may supply nutrients (Figure A1), but this effect could be counterbalanced by strongly freshened nearshore waters (salinity often < 34) and higher turbidity, which reduce light availability; together, these conditions are thought to be less favorable for Sargassum growth. In addition, there is little further advective supply through Cape Palmas because upstream Sargassum west of the cape disappear under the same unfavorable conditions (Figure 6h, discussed in sect. 4.1). The summer decline in Sargassum biomass is strongest in the western Gulf, particularly along the coasts of Ivory Coast  
290 and Ghana, consistent with field observations (e.g., Komoe et al., 2016). In the eastern Gulf (Togo–Benin–Nigeria), by contrast, Sargassum arrive later because of the transit time from Cape Palmas and may remain near the coast, where southerly winds favour retention and stranding, in line with reported observations (Areola et al., 2024; Issifou et al., 2014; Solarin et al., 2014).

Meanwhile, during late summer, the basin-scale circulation sets the stage for the autumn influx. Strengthened southeasterly  
295 trade winds and the monsoon intensify the NECC, which reaches its annual maximum and feeds directly into the GC, itself strongest along the West African coast during the rainy season (Binet, 1997;Djakouré et al., 2024). Because of the three-month advection delay, the coastal Sargassum peaks observed in boreal autumn reflect the strong eastward transport established in late summer across the e-TA. In boreal autumn (September–November), the supply to the n-GoG is therefore fed by Sargassum advected eastward across the basin (Figure 5g). Sargassum accumulate along Guinea and Sierra Leone and are then advected  
300 southeastward by the GC toward Cape Palmas. There, because the coastline changes orientation, the GC partly detaches from the coast and veers slightly southward (Figure 5h), a feature known to reinforce upwelling off Ivory Coast (e.g., Djakouré et al., 2017; Marchal and Picaut, 1977). Combined with prevailing southerly winds that push Sargassum northward (Figure 5i,l), this configuration reduces efficient eastward export and promotes strong coastal accumulation and major strandings in Ivory Coast and Ghana, creating an accumulation area for Sargassum, as illustrated in Figure 7.

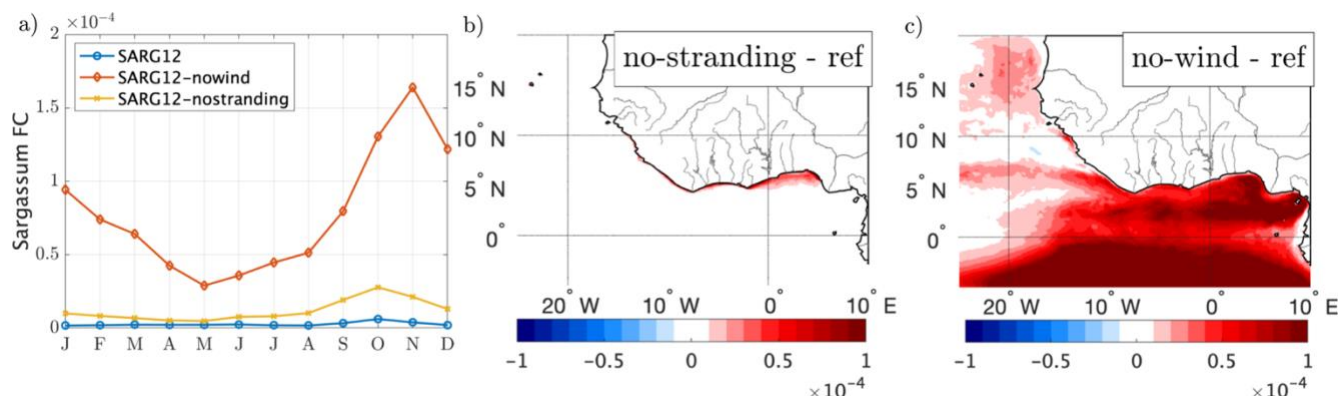
305 Coastal and equatorial upwelling maintain relatively cool, nutrient-enriched surface waters until early autumn (Djakouré et al., 2017, Figure A1), and chlorophyll-a remains elevated after the summer peak (Figure 6l), which supports persistence. By late autumn (November), the ITCZ shifts southward and both the NECC and GC weaken (Figure 5k), reducing further advection; most of the biomass then remains nearshore and strands, consistent with the widespread strandings reported in November. In early winter, reversal of the GC can advect Sargassum northwestward. A persistent biomass often remains offshore of Sierra  
310 Leone and may bloom again in late winter, acting as a seed population for the following season in the Atlantic.



315 Figure 7: Example of the accumulation conditions near Ivory Coast during autumn 2021. Coloured shading shows Sargassum fractional coverage from SARG12 simulation, blue arrows indicate 10 m wind, and black arrows surface currents. The main arrival of Sargassum along the Ivory Coast shelf occur in September–October (b–c). From August (a), strong southerly winds push Sargassum northward toward the coast, where currents weaken in October because GC detaches from the coast (c), favouring retention and accumulation Sargassum along the Ivory Coast shelf until November (d).

### 3.4 Sensitivity of the Sargassum distribution in the GoG to winds and stranding

320 The mechanisms controlling Sargassum accumulation in the n-GoG are further investigated through analysis of sensitivity experiments designed to isolate two key processes: the loss of Sargassum through stranding on the shoreline and the wind-driven transport due to windage and Stokes drift. These experiments allow us to quantify how coastal sinks and wind forcing influence the spatial distribution, persistence, and seasonal cycle of Sargassum reaching the n-GoG.



325 Figure 8: Influence of stranding processes and wind forcing on Sargassum occurrence in the n-GoG. (a) Monthly climatology of mean Sargassum fractional cover in the n-GoG for SARG12 (blue) and the sensitivity experiments SARG12-nostranding (orange) and SARG12-nowind (red). (b-c) Spatial distribution of climatological differences in coastal Sargassum fractional cover between the sensitivity experiments and the reference simulation, showing SARG12-nostranding minus SARG12 (b) and SARG12-nowind minus SARG12 (c). Positive values (red) indicate an increase in Sargassum cover relative to the reference simulation.

### 3.4.1 Effect of stranding

330 In SARG12-nostranding simulation, in which stranding losses are disabled, coastal Sargassum persists much longer in the coastal strip of the GoG because biomass loss at the shoreline is strongly reduced. This appears as a clear shift of the n-GoG distribution toward higher values. Consistently, the seasonal cycle shows that Sargassum remains present for longer in the ocean and decays more slowly after the seasonal peak, whereas in the reference simulation coastal concentrations rapidly decrease once the forcing relaxes and/or the upstream supply weakens (Figure 8a). The difference map further confirms widespread positive anomalies along the n-GoG coastline (Figure 8b), indicating that stranding is a major sink required both to remove coastal Sargassum after the peak seasons and to keep coastal proliferation geographically confined between Ivory Coast and Nigeria (Figure 8b).

335

### 3.4.2 Effect of wind forcing

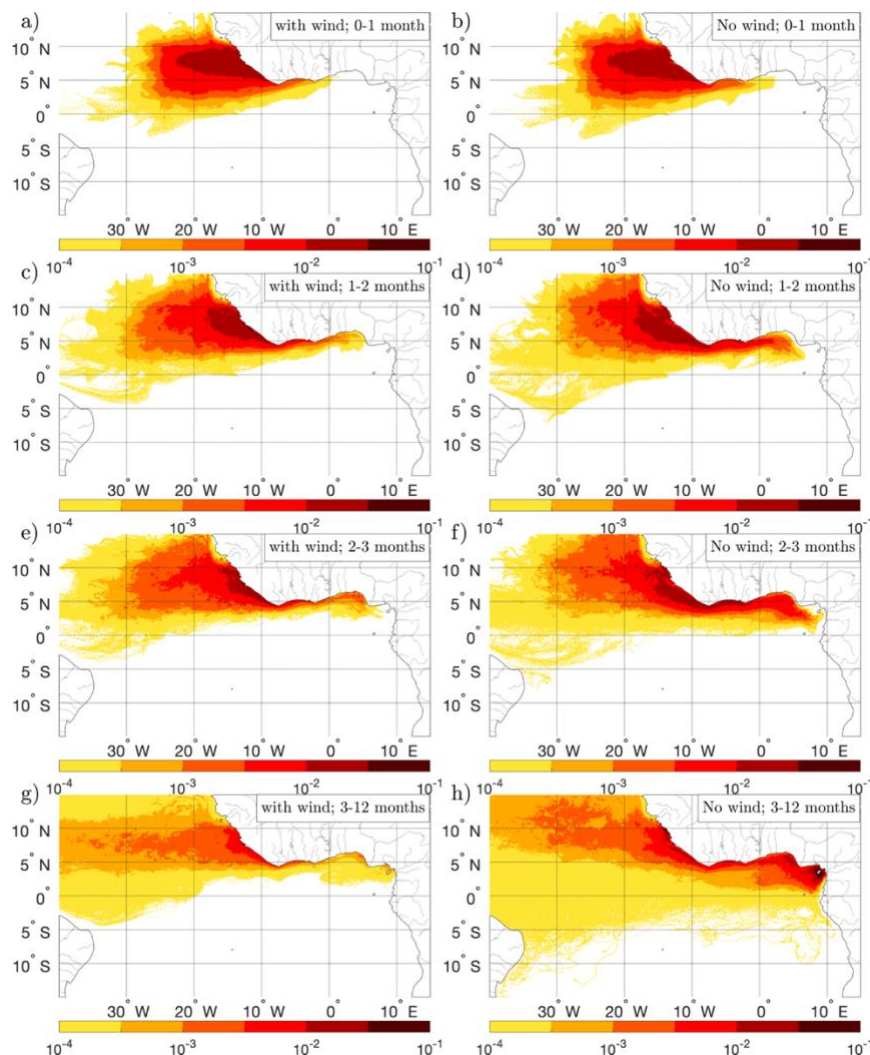
Removing wind forcing (SARG12-nowind run) fundamentally alters circulation of Sargassum. In the e-TA, Sargassum shifts about  $\sim 2^\circ$  southward, highlighting the role of winds in maintaining Sargassum at higher latitudes (Figure 8c). Around Cape Palmas, the absence of wind opposition to the GC also facilitates south-eastward advection. These two factors make the cape cease to act as a selective gateway: Sargassum enters the n-GoG every year, even when western biomass supply is weak, resulting in much higher Sargassum concentration in n-GoG, all year (Figure 8a,c). East of the cape, Sargassum remain embedded in the core of the GC and are advected eastward near  $\sim 4^\circ\text{N}$ , whereas in the wind-forced experiment trajectories are concentrated within a narrower coastal band, with enhanced coastal accumulation and strandings around Cape Palmas (Figure 9). This contrast highlights the role of winds in deflecting Sargassum out of the GC and toward the coast after Cape Palmas, thereby creating the accumulation trap near Ivory Coast and enabling strandings (Section 3.3). Simulated nearshore concentrations along the Ivory Coast–Ghana coast are comparable to those in the reference run despite a much larger basin-

340

345



350 wide biomass (Figure 8c), further emphasizing the regulatory role of stranding on coastal Sargassum abundance. A secondary  
consequence of the absence of winds is the emergence of a southern pathway that is absent in the reference simulation: most  
of the Sargassum continues toward Cameroon, and forward Lagrangian experiment show that part of it turns south along the  
GoG margin and reaches about 5°S before recirculating westward within the SEC (Figure 9h). The southern GoG then becomes  
invaded by Sargassum, where it can proliferate year-round under favourable conditions, leading to a strong increase in biomass  
(Figure 8c). We discuss this pathway further in Section 4.3. Taken together, these results show that wind forcing plays an  
355 essential role in Sargassum circulation by (i) setting the latitudinal position of Sargassum in the e-TA, (ii) enabling  
accumulation along the n-GoG coasts, and (iii) preventing southward propagation that would otherwise lead to basin-wide  
proliferation.



360 Figure 9: Forward trajectory density from the e-TA, shown for four advection-time classes: 0–1 month (a–b), 1–2 months (c–d), 2–3 months (e–f), and 3–12 months (g–h). Left panels show the wind-forced experiment, right panels the no-wind experiment. Colors indicate trajectory density, expressed as the fraction of trajectory occurrences in each  $0.1^\circ \times 0.1^\circ$  grid cell, shown on a logarithmic scale.

### 3.5 Interannual Variability of Coastal Sargassum in the n-GoG

We now examine the main drivers that control the interannual variability of Sargassum arrivals in the n-GoG. To do so, we performed a composite analysis and distinguish spring and autumn seasons.

365

#### 3.5.1 Composite definition

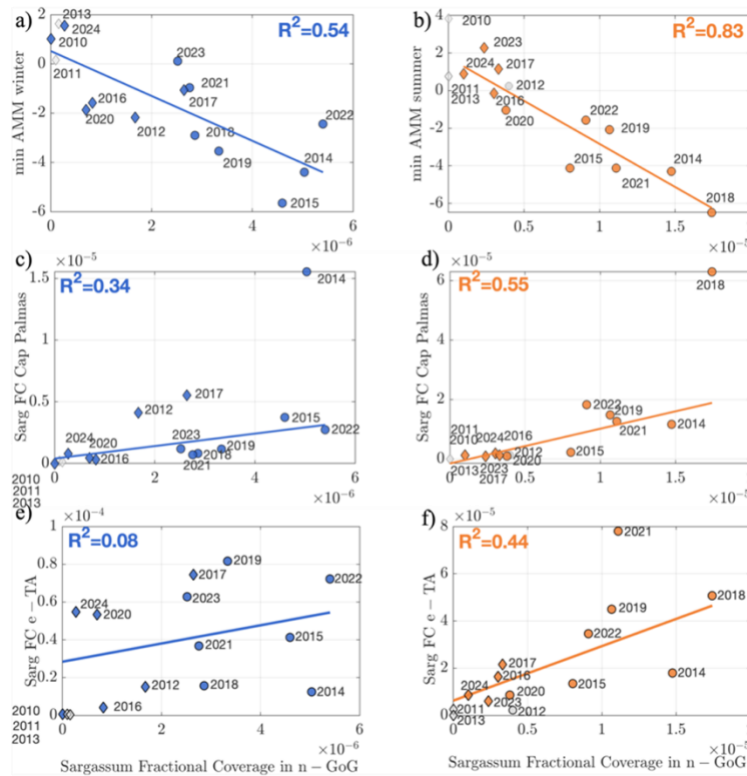
We define “low-Sargassum” and “high-Sargassum” years from SARG12 simulation using a monthly index computed over the n-GoG. First, surface Sargassum fractional cover is averaged monthly over the n-GoG box for the period 2010–2024. High Sargassum years are identified when this monthly mean exceeds its 75th percentile, computed over the full 2010–2024 period.



370 Consecutive above-threshold months within the same season are merged into a single episode. Seasons are defined as winter (December–February), spring (March–June), summer (July–August), and autumn (September–November), although only spring and autumn are analyzed here. Low-Sargassum years are defined as years with mean fractional cover remaining below the threshold throughout the season. Atmospheric and oceanic variables (winds, currents, SST, SSS, nutrients, SSH) are then composited as monthly means.

375 We apply simple time lags consistent with the expected Sargassum advection times estimated from the Lagrangian experiments (Section 3.2). We therefore relate coastal arrivals in the n-GoG at month  $M$  to upstream conditions in the Cape Palmas box one month earlier ( $M - 1$ ), and in the e-TA box two to three months earlier ( $M - 2$  to  $M - 3$ ), in order to account for the delayed influence of transport through the NECC/GC pathway. For the AMM, we retain the minimum value over the six months preceding each event, as this metric was shown to correspond to the southernmost position of Sargassum in the e-TA during  
380 the prevailing season (Figure C1).

The results show that coastal influxes depend primarily on the advection of biomass from the e-TA. Two factors appear to be particularly important: (i) the basin-scale abundance of Sargassum in the e-TA (Figure 10e,f), and (ii) the AMM (Figure 10a,b). By contrast, local environmental conditions within the Gulf, such as salinity and nutrient availability, appear to play only a secondary role, although they may modulate Sargassum survival once established near the coast (Figure D1). Below, we detail  
385 how these factors drive year-to-year differences in Sargassum arrivals during boreal spring (MAM) and autumn (SON).



390

Figure 10: Interannual relationships between coastal Sargassum fractional coverage (FC) in the n-GoG and large-scale controls, for MAM (left) and SON (right). (a, b) Minimum Atlantic Meridional Mode (AMM) index over the preceding 6 months versus coastal FC. (c, d) Cape Palmas FC versus coastal FC. (e, f) Equatorial Sargassum stock in the e-TA versus coastal FC. Coloured symbols indicate years with western supply (blue for MAM, orange for SON), whereas grey symbols indicate years without western supply. Linear regressions and corresponding  $R^2$  values are shown for western-supply years only.

### 3.5.2 Interannual variability in spring

395

The amount of Sargassum reaching the n-GoG in boreal spring is partly determined by the biomass advected across Cape Palmas ( $r^2 = 0.34$ , Figure 10c). This input is strongly correlated with the Sargassum stock along the Sierra Leone–Liberia coast at the end of winter ( $r^2 = 0.83$ , not shown), which is itself conditioned by the intensity of the preceding winter bloom. The AMM plays a key role by modulating the latitudinal position of the offshore Sargassum stock ( $r^2 = 0.54$ , Figure 10a). During negative AMM phases, the ITCZ shifts southward, displacing offshore biomass toward lower latitudes and creating a secondary source of Sargassum between 0 and 5°N as shown by the Lagrangian trajectories experiment (Figure 4). Low AMM conditions also enhance the meridional wind across the equator and thereby strengthen the NECC by about 0.15 m/s on average (Figure 11, right column), favoring the eastward entrainment of the Sargassum. Residual pools near Sierra Leone are also more efficiently advected southward during negative AMM phases, because the ITCZ displacement modifies wind convergence and reduces the Stokes drift and windage that normally oppose the GC (Figure B1).

400



405 Conditions within the Gulf itself appear to be less influential, as indicated by the weak correlations found with other local variables (Figure D1:  $r^2 < 0.12$  for all parameters).

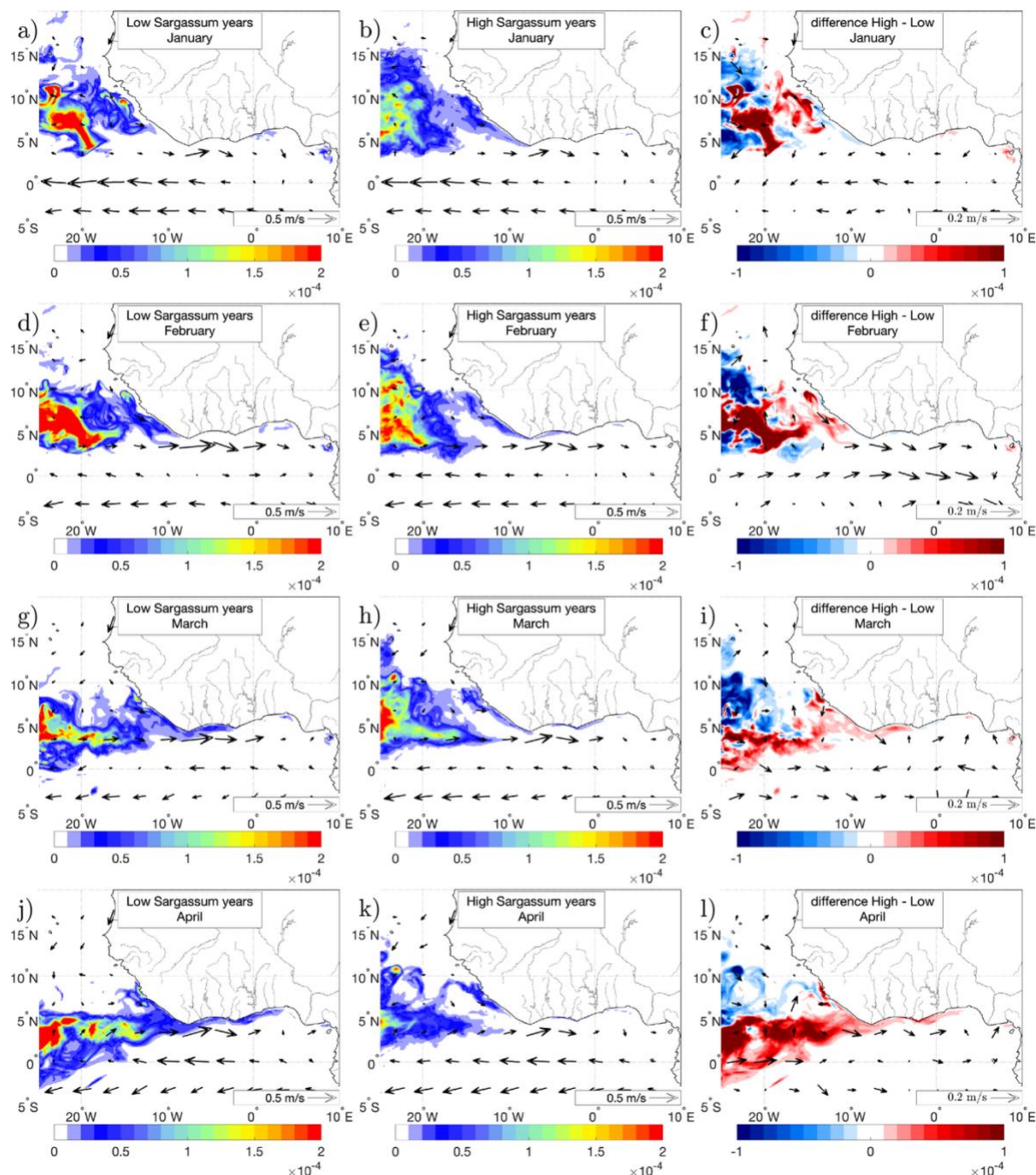


Figure 11: MAM (March–May) composites and contrasts between high- and low-Sargassum years. Seasonal mean Sargassum fractional coverage for January, February, March, and April is shown from top to bottom. The left column shows the high-Sargassum composites, the middle column the low-Sargassum composites, and the right column their difference (high minus low). Surface currents are superimposed in the left and middle columns, while current differences are superimposed in the right column.

410



### 3.5.3 Interannual variability in autumn

In boreal autumn, the AMM appears to be the main large-scale driver of interannual variability in coastal Sargassum arrivals in the n-GoG ( $r^2 = 0.83$ , Figure 10b). The AMM influences this transport in several ways. During negative AMM phases, the ITCZ shifts southward, displacing the Sargassum band to slightly lower latitudes and strengthening the NECC (Figure 12c). These conditions favor eastward advection of the offshore stock toward Cape Palmas and increase the probability that Sargassum converge along the Sierra Leone–Liberia coast before entering the GoG (Figure 12c). At the same time, wind anomalies reduce the northward windage and Stokes drift that would otherwise oppose this transport, although this effect appears secondary (Figure B1). In addition, the AMM also affects the magnitude of the offshore Sargassum stock itself earlier in the year, consistent with the broader link between AMM variability and Sargassum development in the tropical Atlantic (Skiriris et al., 2022). In autumn, the AMM therefore controls both the position and intensity of the upstream reservoir and the efficiency with which this reservoir is advected toward the n-GoG. By comparison, conditions within the Gulf seem to play a secondary role (Figure D1), except possibly near Nigeria, where the persistence of spring Sargassum through summer, as in 2014 and 2017, may provide an additional local biomass source. This is further supported by the relationship at Cape Palmas (Figure 10d): coastal Sargassum in the n-GoG is closely linked to the flux crossing this section ( $r^2 = 0.55$ ), showing that the key control is the amount of offshore biomass advected into the Gulf, not local conditions after entry.

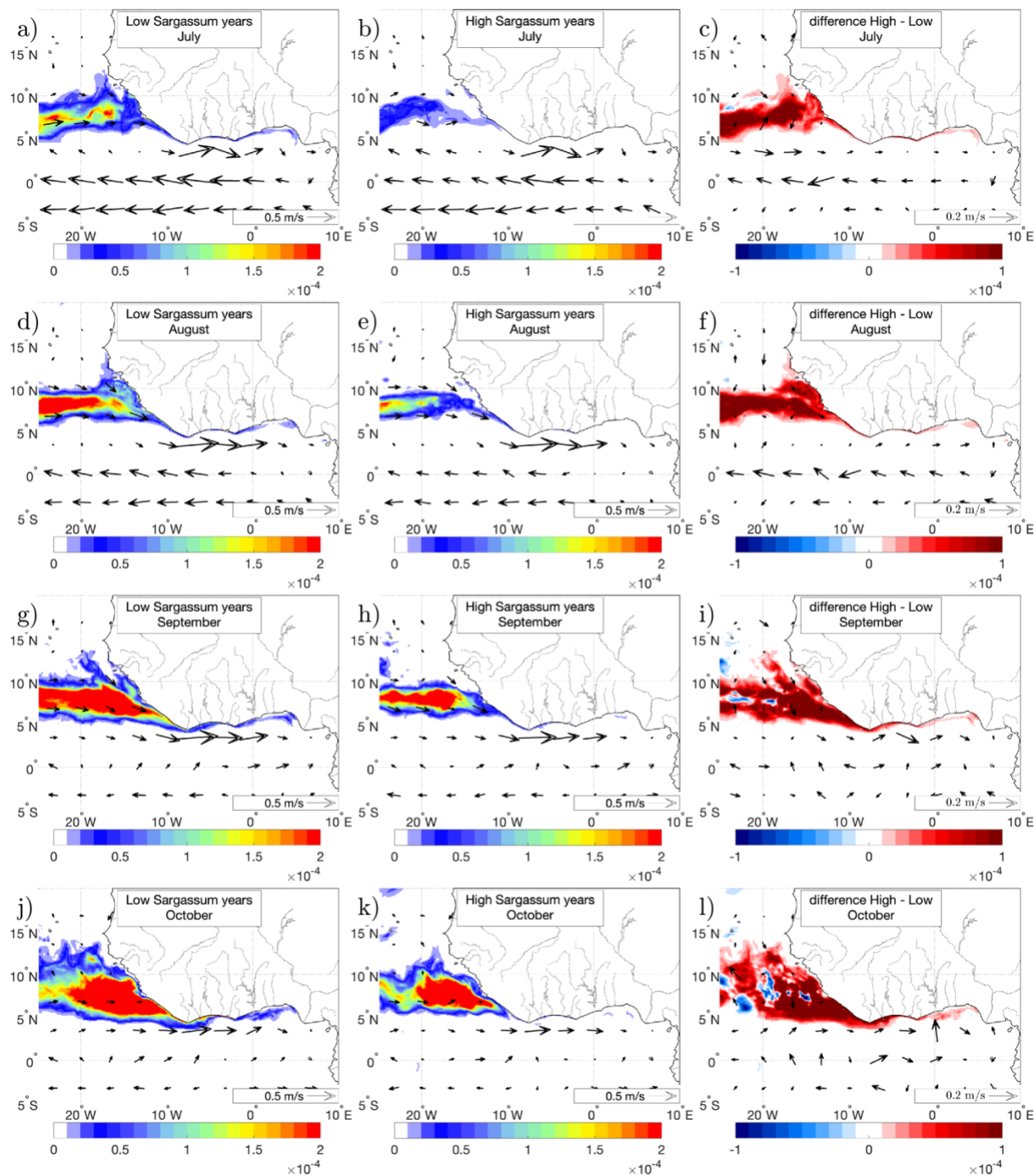


Figure 12: Same as Figure 11, but for autumn (SON)



#### 4. Discussion

430 This study examined the year-to-year drivers of Sargassum arrivals in the n-GoG. Climatologically, two main influx periods  
dominate: spring (MAM) and autumn (SON). In spring, arrivals originate primarily from the winter bloom maintained off the  
Guinea–Sierra Leone coast and along the Sierra Leone–Liberia sector; Sargassum is then transported eastward by the  
developing GC, with a secondary, more southerly offshore source emerging during negative AMM years. In autumn, arrivals  
are mainly fed by large stocks from the e-TA that are advected eastward by a strengthened NECC. Within the n-GoG,  
435 prevailing southerly winds push Sargassum toward the coast, favoring stranding and limiting further southward propagation.  
In SON, Sargassum often accumulates off Ivory Coast under strong southerly winds and weakened nearshore currents (Figure  
7), which retain biomass near the coast. As stranding progressively increases and environmental conditions deteriorate later in  
the season, most of this Sargassum eventually disappears.

Two main factors dominate the interannual signal: (i) the basin-scale Sargassum supply in the tropical Atlantic, and (ii) the  
440 latitudinal position of the Sargassum as they approach the Sierra Leone–Liberia coast, which is controlled by the  
AMM/ITCZ/NECC configuration. The first determines whether a minimum biomass threshold is exceeded; the second  
determines whether Sargassum is steered far enough south to be entrained past Cape Palmas into the n-GoG. Local conditions  
within the Gulf, including salinity, nutrients, windage, and stranding, modulate survival only after these two basin-scale  
controls are met.

445 In autumn (SON), arrivals depend strongly on the AMM: negative AMM phases shift the ITCZ southward, increase meridional  
wind shear, and strengthen the NECC, thereby favoring the positioning and eastward transport of Sargassum along the Sierra  
Leone–Liberia margin toward Cape Palmas. In spring (MAM), arrivals depend mainly on the winter–spring stock already  
present along the Sierra Leone–Liberia coast, which is set by the preceding winter bloom and downstream retention. A low  
AMM may also establish a secondary Sargassum source within the ITCZ, increasing the offshore biomass available for  
450 transport toward the Gulf. Yet because the ITCZ is already climatologically located far south in late winter and spring,  
advection around Cape Palmas is generally favourable during this season, making the AMM a secondary rather than dominant  
control.

##### 4.1 Sargassum persistence off Sierra Leone and the role of the winter bloom

Observational and modelling studies identify the Sierra Leone–Guinea sector as a recurrent winter reservoir of Sargassum that  
455 seeds the subsequent spring influx and, through recirculation, contributes to the wider Atlantic belt (Berline et al., 2020; Johns  
et al., 2020; Wang et al., 2019, Jouanno et al. 2025a). Basin-scale satellite climatologies and back-trajectory analyses show a  
buildup of biomass in the eastern and central tropical Atlantic from late winter into spring, with downstream retention off  
Guinea and Sierra Leone and subsequent export both westward and eastward as the NECC strengthens seasonally.

Several mechanisms may explain the late-spring to summer decline of the bloom in the Guinea–Sierra Leone region. First,  
460 regional upwelling relaxes from late spring into summer and autumn, reducing the supply of nutrient-rich subsurface waters



and therefore limiting growth potential (Binet, 1997; Djakouré et al., 2017). Second, the peak of the West African monsoon brings intense rainfall that freshens coastal waters from July onward, with salinity frequently below 34 (Thouvenin-Masson et al., 2024) and increase turbidity, creating less favourable conditions for Sargassum survival. Although rainfall and river discharge may also enhance nutrient inputs, the strongest river outflows generally occur in autumn, so this effect may not  
465 compensate for the adverse summer conditions. Third, the monsoon wind-wave regime may increase mortality through fragmentation and enhanced stranding (Laval et al., 2025).

#### 4.2 The future of Sargassum arrivals in the n-GoG

Regarding long-term evolution, three points emerge from the literature. First, the tropical Atlantic Sargassum baseline has remained higher since 2011, which by itself increases the likelihood that seasonal biomass exceeds the supply threshold and  
470 therefore raises the risk of n-GoG invasion (Berline et al., 2020; Johns et al., 2020; Wang et al., 2019). Second, forced trends in the AMM/ITCZ background state over the Atlantic remain uncertain: theory and models suggest a narrowing and meridional shift of the tropical rain belt, whose sign over the Atlantic depends on aerosol forcing, hemispheric energy contrasts, and AMOC changes (Byrne et al., 2018; Calvin et al., 2023; Donohoe et al., 2013; Hwang and Frierson, 2013). A tendency toward  
475 a more northerly mean ITCZ would reduce the frequency of negative AMM-like seasons, and which are favourable to a weakening of Sargassum delivery into the n-GoG, whereas a southward displacement of the ITCZ, for example under a weakened AMOC, would favour the transport of the Sargassum in the GoG. Future n-GoG inundation risk will therefore depend on the combined evolution of (i) the basin-wide Sargassum baseline, likely to remain higher than before 2011, and (ii) the frequency of negative AMM configurations.

#### 4.3 Southern (“SEC”) export pathway

A southward export pathway from the GoG into the SEC, and then toward northeastern Brazil and occasionally back into the NECC, has been proposed from drifter syntheses and connectivity analyses (Beron-Vera et al., 2022; Franks et al., 2016; Johns et al., 2020). In our reference simulations, however, this pathway does not emerge as a robust feature. Strong southerly monsoon winds and wave-driven drift trap Sargassum against the n-GoG coast, while downstream losses through stranding and senescence east of Cape Palmas further reduce the likelihood of coherent export south of the Equator. By contrast, the  
485 SEC branch does emerge in our no-wind experiment, indicating that wind drift is the main barrier to this route. Additional idealized Lagrangian advection experiments both with and without wind forcing (Figure 9) further support this interpretation. They show that some trajectories can cross into the Southern Hemisphere and seed the southern Gulf of Guinea, where environmental conditions may then become favourable for Sargassum proliferation, whereas this southward pathway is strongly reduced when wind forcing is included. The SEC pathway may therefore be considered conditional: it may become  
490 active only under unusually large biomass surpluses in the n-GoG or under anomalous alongshore wind conditions, but it does not appear to represent a common present-day pathway for Sargassum.



Satellite observations also provide little support for this pathway, since any southward leakage would likely take the form of thin, low-fraction filaments that are difficult to detect under the persistent cloud cover of JJA–SON. Although some satellite composites occasionally indicate floating material near the Congo River mouth, we found no peer-reviewed field reports confirming Sargassum there. Given the high turbidity and CDOM of the Congo plume, these signals are likely affected by false detections, consistent with the known limitations of ocean-colour Sargassum retrievals in optically complex waters.

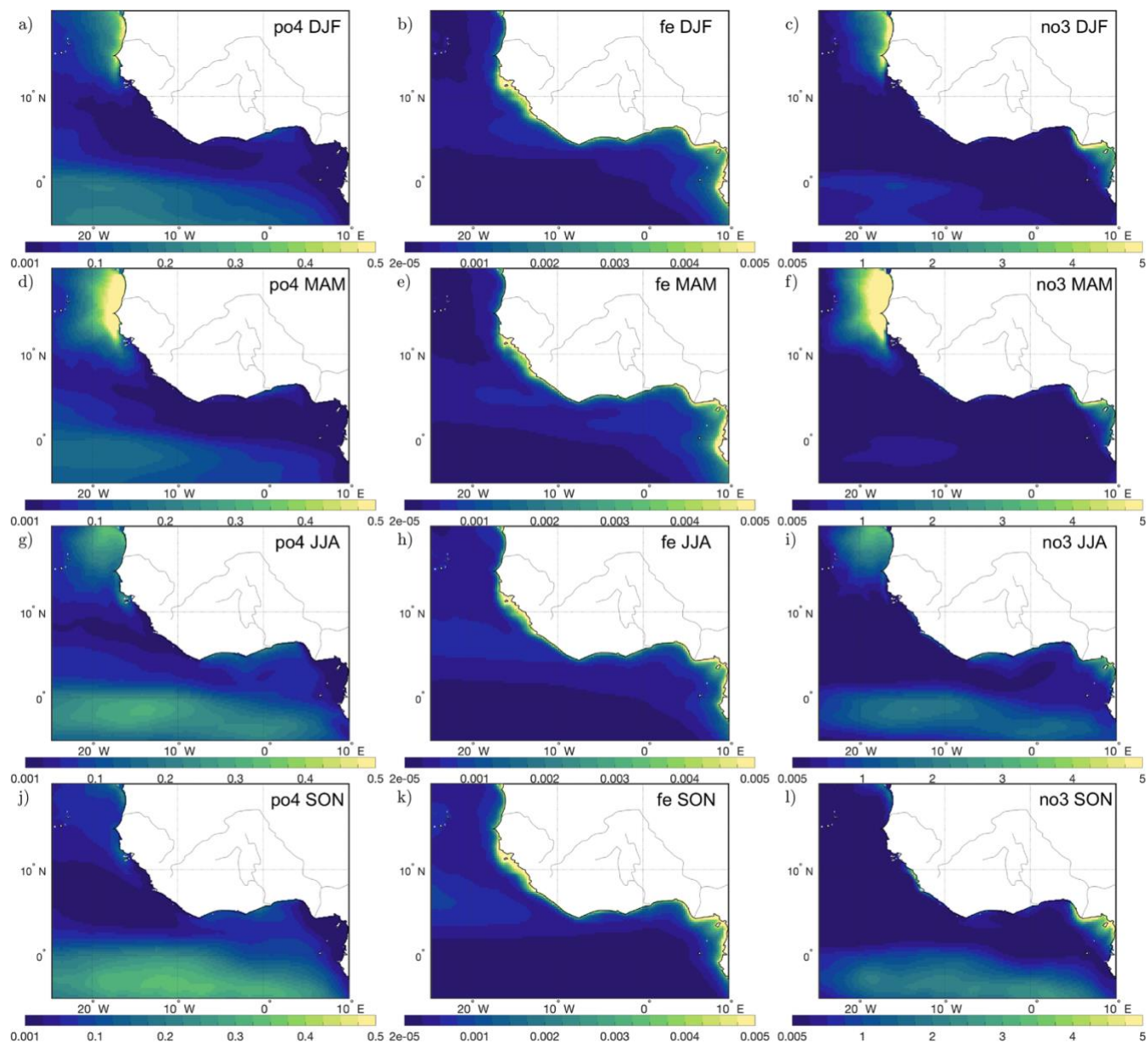
**Author contribution:** CTM and JJ designed the experiments and CTM carried them out. JJ developed the model code and performed the simulations. CTM prepared the manuscript with contributions from JJ.

**Competing interests:** The authors declare that they have no conflict of interest.

**Financial support:** This study was supported by CNES, through project TOSCA SARGAT under grants 10035 and 10513. Computing resources are provided by GENCI under grant GEN7298

**Data availability statement:** The Atlantic Meridional Mode (AMM) index, computed from SST anomalies in the tropical Atlantic following the definition of (Chiang and Vimont, 2004). We use indices distributed by NOAA (<https://www.aoml.noaa.gov/phod/research/tav/tcv/amm/>, last access 17/09/2025). The Sargassum areal coverage database was processed by AERIS/ICARE data center at the University of Lille and is available at Berline and Desclotres (2021). The BIO4 biogeochemical simulations are available at Mercator Ocean International (2023). GLORYS12 can be downloaded at <https://data.marine.copernicus.eu>. The Sargassum model is built upon the standard NEMO code (release 4.0.1, rev 11533), provided by Madec and the NEMO System Team (2023). The NEMO code modified to include the Sargassum physiology and transport is available in the Zenodo archive at Jouanno and Benshila (2020).

Appendix A



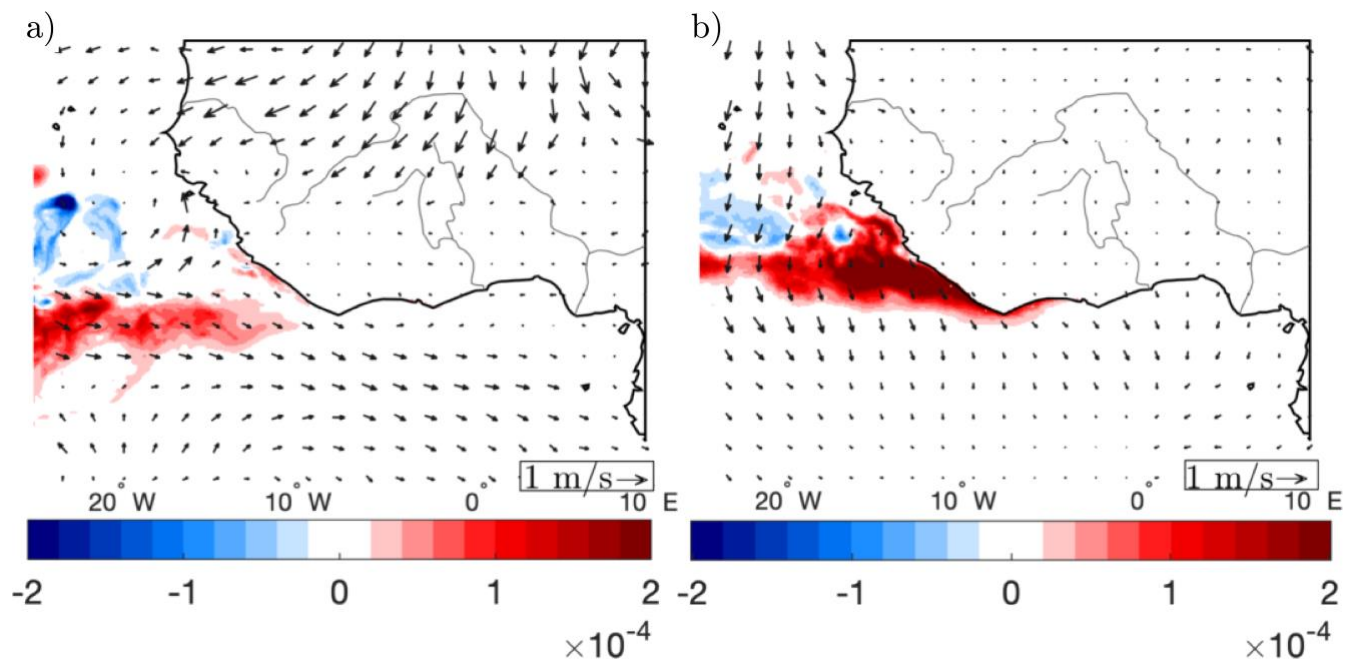
515

Figure A1: Seasonal climatologies of the biogeochemical surface environment in the eastern tropical Atlantic and Gulf of Guinea, averaged over all years of the analysis period. From left to right: phosphate, iron, and chlorophyll. From top to bottom: boreal winter (DJF), spring (MAM), summer (JJA), and autumn (SON). These fields provide the seasonal biogeochemical context potentially favorable to *Sargassum* development and maintenance upstream of the Gulf of Guinea.

520



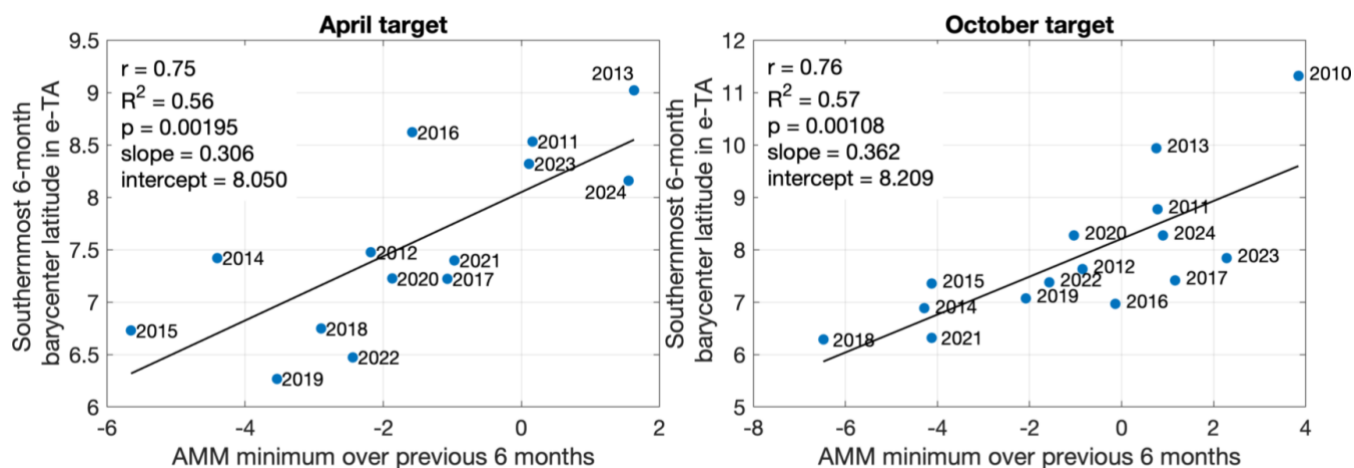
Appendix B



525 Figure B1: Difference of Sargassum quantities (colors) and difference of wind forcing between years with Sargassum and years with few Sargassum in n-GoG, during spring (a) and autumn (b).



Appendix C

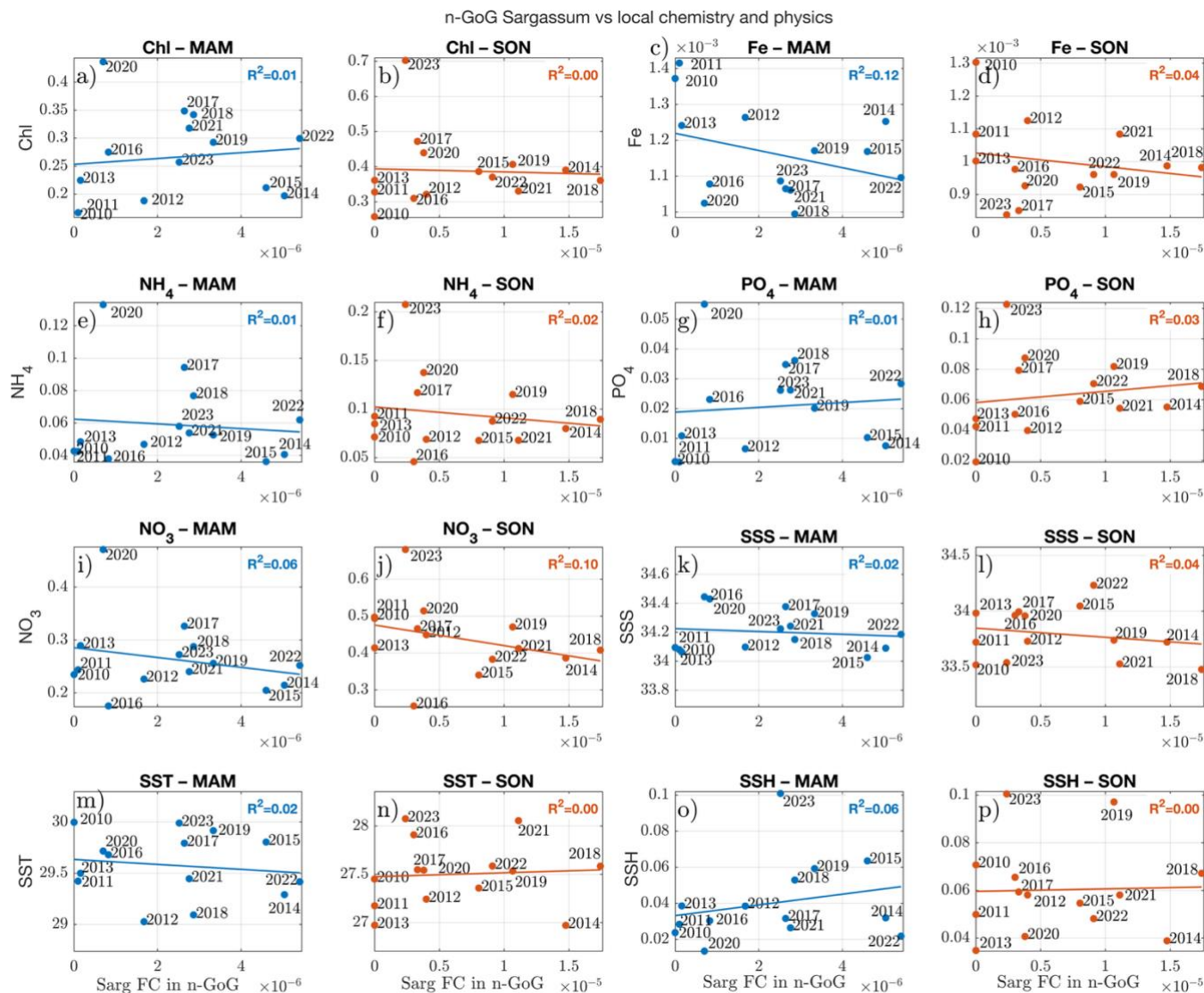


530 Figure C1: Relationship between the minimum Atlantic Meridional Mode (AMM) index over the six months preceding the target month and the southernmost position of Sargassum in the eastern tropical Atlantic, estimated here from the latitude of the southernmost 6-month barycenter. Left: April target (AMM minimum over October–March). Right: October target (AMM minimum over April–September). Each point corresponds to one year, with the year indicated next to the marker. The black line shows the linear regression, and the corresponding statistics are reported in each panel.

535



Appendix D



540 Figure D1: Relationships between coastal Sargassum fractional coverage (FC) in the northern (n-GoG) and local biogeochemical and physical conditions, for MAM (left column of each pair) and SON (right column of each pair). Rows show chlorophyll (Chl), dissolved iron (Fe), ammonium (NH<sub>4</sub>), phosphate (PO<sub>4</sub>), nitrate (NO<sub>3</sub>), sea surface salinity (SSS), sea surface temperature (SST), and sea surface height (SSH). Each marker corresponds to one year (2010–2023), labeled by year. Solid lines indicate linear regressions, and the corresponding R<sup>2</sup> values are given in each panel.

545



## References

- Ackah-Baidoo, A.: Fishing in troubled waters: oil production, seaweed and community-level grievances in the Western Region of Ghana, *Community Development Journal*, 48, 406–420, <https://doi.org/10.1093/cdj/bst022>, 2013.
- 550 Addico, G. N. D. and deGraft-Johnson, K. A. A.: Preliminary investigation into the chemical composition of the invasive brown seaweed *Sargassum* along the west coast of Ghana, *Afr. J. Biotechnol.*, 15, 2184–2191, <https://doi.org/10.5897/AJB2015.15177>, 2016.
- Adet, L., Nsofor, G. N., Ogunjobi, K. O., and Camara, B.: Knowledge of Climate Change and the Perception of Nigeria's Coastal Communities on the Occurrence of *Sargassum natans* and *Sargassum fluitans*, *OALib*, 04, 1–18, 555 <https://doi.org/10.4236/oalib.1104198>, 2017.
- AKA, K. S., SANKARE, Y., KOMOE, K., and N'CHO, A. J.: Influence des algues sargasses (*sargassum fluitans*, *sargassum natans*, *sargassum natans*) sur les activités socio-économiques le long du littoral ivoirien (Côte d'Ivoire – Afrique de l'ouest), *Revue canadienne de géographie tropicale/Canadian journal of tropical geography*, 5, 10–15, 2018.
- Akrong, M. O., Anning, A. K., Addico, G. N. D., deGraft-Johnson, K. A. A., Adu-Gyamfi, A., Ale, M., and Meyer, A. S.: 560 Spatio-temporal variations in seaweed diversity and abundance of selected coastal areas in Ghana, *Regional Studies in Marine Science*, 44, 101719, <https://doi.org/10.1016/j.rsma.2021.101719>, 2021.
- Amorim, J. P. M. D., Carmo, A. M. C. D., and Martinelli Filho, J. E.: *Sargassum* transport to the Amazon Coast: Explaining the stranding through meteorological and oceanographic conditions, *Harmful Algae*, 149, 102955, <https://doi.org/10.1016/j.hal.2025.102955>, 2025a.
- 565 Amorim, J. P. M. D., Carmo, A. M. C. D., and Martinelli Filho, J. E.: *Sargassum* transport to the Amazon Coast: Explaining the stranding through meteorological and oceanographic conditions, *Harmful Algae*, 149, 102955, <https://doi.org/10.1016/j.hal.2025.102955>, 2025b.
- Areola, F., Osanyinlusi, O., and Soyinka, O.: THE BENEFITS AND CHALLENGES OF SARGASSUM SEAWEED TO THE LOCAL FISHING COMMUNITIES IN NIGERIA, *JRRS*, 11, <https://doi.org/10.36108/jrrslasu/4202.11.0102>, 2024.
- 570 Azcorra-May, K. J., Olguin-Maciel, E., Domínguez-Maldonado, J., Toledano-Thompson, T., Leal-Bautista, R. M., Alzate-Gaviria, L., and Tapia-Tussell, R.: *Sargassum* biorefineries: potential opportunities towards shifting from wastes to products, *Biomass Conv. Bioref.*, <https://doi.org/10.1007/s13399-022-02407-2>, 2022.
- Berline, L., Ody, A., Jouanno, J., Chevalier, C., André, J.-M., Thibaut, T., and Ménard, F.: Hindcasting the 2017 dispersal of *Sargassum* algae in the Tropical North Atlantic, *Marine Pollution Bulletin*, 158, 575 <https://doi.org/10.1016/j.marpolbul.2020.111431>, 2020.
- Bernard, D. C., Biabiany, E., Cécé, R., Chery, R., and Sekkat, N.: Clustering analysis of the *Sargassum* transport process: application to stranding prediction in the Lesser Antilles, *Surface/Analytic Theory/Caribbean/Transports/cycling (nutrients, C, O, etc.)/Harmful algae*, <https://doi.org/10.5194/os-2021-109>, 2021.
- 580 Beron-Vera, F. J., Olascoaga, M. J., Putman, N. F., Triñanes, J., Goni, G. J., and Lumpkin, R.: Dynamical geography and transition paths of *Sargassum* in the tropical Atlantic, *AIP Advances*, 12, 105107, <https://doi.org/10.1063/5.0117623>, 2022.
- Berthet, S., Sférian, R., Bricaud, C., Chevallier, M., Voltaire, A., and Ethé, C.: Evaluation of an Online Grid-Coarsening Algorithm in a Global Eddy-Admitting Ocean Biogeochemical Model, *J Adv Model Earth Syst*, 11, 1759–1783, <https://doi.org/10.1029/2019MS001644>, 2019.



- 585 Binet, D.: Climate and pelagic fisheries in the Canary and Guinea currents 1964–1993 : the role of trade winds and the southern oscillation, *Oceanologica Acta*, 20, 177–190, 1997.
- Brooks, M. T., Coles, V. J., Hood, R. R., and Gower, J. F. R.: Factors controlling the seasonal distribution of pelagic Sargassum, *Mar. Ecol. Prog. Ser.*, 599, 1–18, <https://doi.org/10.3354/meps12646>, 2018.
- Byrne, M. P., Pendergrass, A. G., Rapp, A. D., and Wodzicki, K. R.: Response of the Intertropical Convergence Zone to Climate Change: Location, Width, and Strength, *Curr Clim Change Rep*, 4, 355–370, <https://doi.org/10.1007/s40641-018-0110-5>, 2018.
- 590 Calvin, K., Dasgupta, D., Krinner, G., Mukherji, A., Thorne, P. W., Trisos, C., Romero, J., Aldunce, P., Barrett, K., Blanco, G., Cheung, W. W. L., Connors, S., Denton, F., Diongue-Niang, A., Dodman, D., Garschagen, M., Geden, O., Hayward, B., Jones, C., Jotzo, F., Krug, T., Lasco, R., Lee, Y.-Y., Masson-Delmotte, V., Meinshausen, M., Mintenbeck, K., Mokssit, A., Otto, F. E. L., Pathak, M., Pirani, A., Poloczanska, E., Pörtner, H.-O., Revi, A., Roberts, D. C., Roy, J., Ruane, A. C., Skea, J., Shukla, P. R., Slade, R., Slangen, A., Sokona, Y., Sörensson, A. A., Tignor, M., Van Vuuren, D., Wei, Y.-M., Winkler, H., Zhai, P., Zommers, Z., Hourcade, J.-C., Johnson, F. X., Pachauri, S., Simpson, N. P., Singh, C., Thomas, A., Totin, E., Arias, P., Bustamante, M., Elgizouli, I., Flato, G., Howden, M., Méndez-Vallejo, C., Pereira, J. J., Pichs-Madruga, R., Rose, S. K., Saheb, Y., Sánchez Rodríguez, R., Ürgé-Vorsatz, D., Xiao, C., Yassaa, N., Alegría, A., Armour, K., Bednar-Friedl, B., Blok, K., Cissé, G., Dentener, F., Eriksen, S., Fischer, E., Garner, G., Guivarch, C., Haasnoot, M., Hansen, G., Hauser, M., Hawkins, E., Hermans, T., Kopp, R., Leprince-Ringuet, N., Lewis, J., Ley, D., Ludden, C., Niamir, L., Nicholls, Z., Some, S., Szopa, S., Trewin, B., Van Der Wijst, K.-I., Winter, G., Witting, M., Birt, A., Ha, M., et al.: IPCC, 2023: Climate Change 2023: Synthesis Report. Contribution of Working Groups I, II and III to the Sixth Assessment Report of the Intergovernmental Panel on Climate Change [Core Writing Team, H. Lee and J. Romero (eds.)]. IPCC, Geneva, Switzerland., Intergovernmental Panel on Climate Change (IPCC), <https://doi.org/10.59327/IPCC/AR6-9789291691647>, 2023.
- 600 Carpenter, E. J. and Cox, J. L.: Production of pelagic Sargassum and a blue-green epiphyte in the western Sargasso Sea, *Limnol. Oceanogr.*, 19, 429–436, <https://doi.org/10.4319/lo.1974.19.3.0429>, 1974.
- Chávez, V., Uribe-Martínez, A., Cuevas, E., Rodríguez-Martínez, R. E., van Tussenbroek, B. I., Francisco, V., Estévez, M., Celis, L. B., Monroy-Velázquez, L. V., Leal-Bautista, R., Álvarez-Filip, L., García-Sánchez, M., Masia, L., and Silva, R.: Massive Influx of Pelagic Sargassum spp. on the Coasts of the Mexican Caribbean 2014–2020: Challenges and Opportunities, *Water*, 12, 2908, <https://doi.org/10.3390/w12102908>, 2020.
- 610 Chiang, J. C. H. and Vimont, D. J.: Analogous Pacific and Atlantic Meridional Modes of Tropical Atmosphere–Ocean Variability\*, *Journal of Climate*, 17, 4143–4158, <https://doi.org/10.1175/JCLI4953.1>, 2004.
- Delandmeter, P. and Van Sebille, E.: The Parcels v2.0 Lagrangian framework: new field interpolation schemes, *Geosci. Model Dev.*, 12, 3571–3584, <https://doi.org/10.5194/gmd-12-3571-2019>, 2019a.
- 615 Delandmeter, P. and Van Sebille, E.: The Parcels v2.0 Lagrangian framework: new field interpolation schemes, *Geosci. Model Dev.*, 12, 3571–3584, <https://doi.org/10.5194/gmd-12-3571-2019>, 2019b.
- Descloitres, J., Minghelli, A., Steinmetz, F., Chevalier, C., Chami, M., and Berline, L.: Revisited Estimation of Moderate Resolution Sargassum Fractional Coverage Using Decametric Satellite Data (S2-MSI), *Remote Sensing*, 13, 5106, <https://doi.org/10.3390/rs13245106>, 2021.
- 620 DGEC and MCVDD: État de l’environnement marin du Bénin, DGEC, Cotonou, Bénin, 2020.



- Dirisu, A.-R., Uyi, H. S., and Uyi, M.: First report on the occurrence of Sargassum Weed Fish *Histrio histrio* (Lophiliiformes: Antennariidae) in Nigeria deep water, Gulf of Guinea, *J. Threat. Taxa*, 13, 18899–18902, <https://doi.org/10.11609/jott.4413.13.7.18899-18902>, 2021.
- 625 Djakouré, S., Penven, P., Bourlès, B., Koné, V., and Veitch, J.: Respective Roles of the Guinea Current and Local Winds on the Coastal Upwelling in the Northern Gulf of Guinea, *Journal of Physical Oceanography*, 47, 1367–1387, <https://doi.org/10.1175/JPO-D-16-0126.1>, 2017.
- Djakouré, S., Konaté, Y., Koné, V., Bosson, K., Koné, M., and Kouadio, K. Y.: Relationship between the Guinea Current and the Coastal Upwelling in Northern of Gulf of Guinea, *OJMS*, 14, 63–77, <https://doi.org/10.4236/ojms.2024.144004>, 2024.
- 630 Donohoe, A., Marshall, J., Ferreira, D., and Mcgee, D.: The Relationship between ITCZ Location and Cross-Equatorial Atmospheric Heat Transport: From the Seasonal Cycle to the Last Glacial Maximum, *Journal of Climate*, 26, 3597–3618, <https://doi.org/10.1175/JCLI-D-12-00467.1>, 2013.
- Environment Protection Agency: Sierra Leone State of the Marine Environment report 2015, Freetown, Sierra Leone., 2015.
- Fidai, Y. A., Donnelly, J., Tompkins, E. L., and Tonon, T.: A systematic review of floating and beach landing records of Sargassum beyond the Sargasso Sea, *Environ. Res. Commun.*, 2, 122001, <https://doi.org/10.1088/2515-7620/abd109>, 2020.
- 635 Fidai, Y. A., Dash, J., Marsh, R., Oxenford, H. A., Biermann, L., Martin, N., and Tompkins, E. L.: Tracking and detecting sargassum pathways across the tropical Atlantic, *Environ. Res. Commun.*, 5, 125010, <https://doi.org/10.1088/2515-7620/ad14a3>, 2023.
- Fidai, Y. A., Dash, J., Tompkins, E., Atiglo, D. Y., Jayson-Quashigah, P.-N., Sowah, W. N. A., and Addo, K. A.: Sargassum Biomass Movement and Proliferation in the Eastern Tropical Atlantic, *Phycology*, 5, 17, <https://doi.org/10.3390/phycology5020017>, 2025.
- 640 Franks, J. S., Johnson, D. R., Ko, D.-S., Sanchez-Rubio, G., Hendon, J. R., and Lay, M.: Unprecedented influx of pelagic Sargassum along Caribbean island coastlines during summer 2011, in: 64th Gulf and Caribbean Fisheries Institute, Gulf and Caribbean Fisheries Institute Conference, 6–8, 2012.
- Franks, J. S., Johnson, D. R., and Ko, D. S.: Pelagic Sargassum in the tropical North Atlantic, *GCR*, 27, <https://doi.org/10.18785/gcr.2701.08>, 2016.
- 645 Gobert, T., Connan, S., Johnson, D. R., and Waeles, M.: The Guiana current: a fast-lane to the Caribbean for holopelagic Sargassum contaminated in arsenic and cadmium, *Harmful Algae*, 150, 102981, <https://doi.org/10.1016/j.hal.2025.102981>, 2025.
- Gower, J., Young, E., and King, S.: Satellite images suggest a new Sargassum source region in 2011, *Remote Sensing Letters*, 4, 764–773, <https://doi.org/10.1080/2150704X.2013.796433>, 2013.
- 650 Grodsky, S. A. and Carton, J. A.: The Intertropical Convergence Zone in the South Atlantic and the Equatorial Cold Tongue, *J. Climate*, 16, 723–733, [https://doi.org/10.1175/1520-0442\(2003\)016%253C0723:TICZIT%253E2.0.CO;2](https://doi.org/10.1175/1520-0442(2003)016%253C0723:TICZIT%253E2.0.CO;2), 2003.
- Hardman-Mountford, N. J. and McGlade, J. M.: 5 Variability of physical environmental processes in the gulf of guinea and implications for fisheries recruitment. An investigation using remotely sensed SST, in: *Large Marine Ecosystems*, vol. 11, Elsevier, 49–xxviii, [https://doi.org/10.1016/S1570-0461\(02\)80027-1](https://doi.org/10.1016/S1570-0461(02)80027-1), 2002.
- 655



- 660 Hersbach, H., Bell, B., Berrisford, P., Hirahara, S., Horányi, A., Muñoz-Sabater, J., Nicolas, J., Peubey, C., Radu, R., Schepers, D., Simmons, A., Soci, C., Abdalla, S., Abellan, X., Balsamo, G., Bechtold, P., Biavati, G., Bidlot, J., Bonavita, M., De Chiara, G., Dahlgren, P., Dee, D., Diamantakis, M., Dragani, R., Flemming, J., Forbes, R., Fuentes, M., Geer, A., Haimberger, L., Healy, S., Hogan, R. J., Hólm, E., Janisková, M., Keeley, S., Laloyaux, P., Lopez, P., Lupu, C., Radnoti, G., De Rosnay, P., Rozum, I., Vamborg, F., Villaume, S., and Thépaut, J.: The ERA5 global reanalysis, *Quart J Royal Meteor Soc*, 146, 1999–2049, <https://doi.org/10.1002/qj.3803>, 2020.
- Hwang, Y.-T. and Frierson, D. M. W.: Link between the double-Intertropical Convergence Zone problem and cloud biases over the Southern Ocean, *Proc. Natl. Acad. Sci. U.S.A.*, 110, 4935–4940, <https://doi.org/10.1073/pnas.1213302110>, 2013.
- 665 Issifou, L., Atanle, K., Radji, R., Lawson, H. L., Adjonou, K., Etorh, M. T., Kokutse, A. D., Mensah, A. A., and Kokou, K.: Checklist of tropical algae of Togo in the Guinean Gulf of West-Africa, *Sci. Res. Essays*, 9, 932–958, <https://doi.org/10.5897/SRE2014.6113>, 2014.
- Johns, E. M., Lumpkin, R., Putman, N. F., Smith, R. H., Muller-Karger, F. E., T. Rueda-Roa, D., Hu, C., Wang, M., Brooks, M. T., Gramer, L. J., and Werner, F. E.: The establishment of a pelagic Sargassum population in the tropical Atlantic: Biological consequences of a basin-scale long distance dispersal event, *Progress in Oceanography*, 182, 102269, <https://doi.org/10.1016/j.pocean.2020.102269>, 2020.
- 670 Jouanno, J., Benschila, R., Berline, L., Soulié, A., Radenac, M.-H., Morvan, G., Diaz, F., Sheinbaum, J., Chevalier, C., Thibaut, T., Changeux, T., Menard, F., Berthet, S., Aumont, O., Ethé, C., Nabat, P., and Mallet, M.: A NEMO-based model of *Sargassum* distribution in the tropical Atlantic: description of the model and sensitivity analysis (NEMO-Sarg1.0), *Geosci. Model Dev.*, 14, 4069–4086, <https://doi.org/10.5194/gmd-14-4069-2021>, 2021.
- 675 Jouanno, J., Morvan, G., Berline, L., Benschila, R., Aumont, O., Sheinbaum, J., and Ménard, F.: Skillful Seasonal Forecast of *Sargassum* Proliferation in the Tropical Atlantic, *Geophysical Research Letters*, 50, e2023GL105545, <https://doi.org/10.1029/2023GL105545>, 2023.
- Jouanno, J., Berthet, S., Muller-Karger, F., Aumont, O., and Sheinbaum, J.: An extreme North Atlantic Oscillation event drove the pelagic Sargassum tipping point, *Commun Earth Environ*, 6, 1–11, <https://doi.org/10.1038/s43247-025-02074-x>, 2025a.
- 680 Jouanno, J., Almar, R., Muller-Karger, F., Morvan, G., Van Tussenbroek, B., Benschila, R., Marchesiello, P., and Addo, K. A.: Socio-ecological vulnerability assessment to Sargassum arrivals, *Sci Rep*, 15, 9998, <https://doi.org/10.1038/s41598-025-94475-3>, 2025b.
- 685 Komoe, K., Sankare, Y., Fofie, N. B. Y., Bamba, A., and Sahr, A. G.-S.: Taxonomic study of two species of Sargassum: *Sargassum fluitans* (Borgesien) Borgesien and *Sargassum natans* (Linnaneus) Gaillon (brown algae) collected in Côte d’Ivoire coasts, West Africa, *Nature and Science*, 14, 50–56, 2016.
- Laval, M., Aimene, Y., Descloîtres, J., Courtrai, L., Duarte-Neto, P., Salazar-Garibay, A., Costa Da Silva, A., Zongo, P., Dorville, R., and Chevalier, C.: The Influence of Wind on the Spatial Distribution of Pelagic Sargassum Aggregations in the Tropical Atlantic, *Water*, 17, 776, <https://doi.org/10.3390/w17060776>, 2025.
- 690 Lellouche, J.-M., Eric, G., Romain, B.-B., Gilles, G., Angélique, M., Marie, D., Clément, B., Mathieu, H., Olivier, L. G., Charly, R., Tony, C., Charles-Emmanuel, T., Florent, G., Giovanni, R., Mounir, B., Yann, D., and Pierre-Yves, L. T.: The Copernicus Global 1/12° Oceanic and Sea Ice GLORYS12 Reanalysis, *Front. Earth Sci.*, 9, 698876, <https://doi.org/10.3389/feart.2021.698876>, 2021.
- León-Pérez, M. C., McLaughlin, R., Chaparro, R., Krimsky, L., Klein, Z., Myers, A., and Ankersen, T. T.: Massive influxes of Pelagic Sargassum in the Wider Caribbean Region, *National Sea Grant Law Center.*, 2021.



695 López Miranda, J. L., Celis, L. B., Estévez, M., Chávez, V., van Tussenbroek, B. I., Uribe-Martínez, A., Cuevas, E., Rosillo Pantoja, I., Masia, L., Cauich-Kantun, C., and Silva, R.: Commercial Potential of Pelagic Sargassum spp. in Mexico, *Front. Mar. Sci.*, 8, 768470, <https://doi.org/10.3389/fmars.2021.768470>, 2021.

Maneein, S., Milledge, J. J., Harvey, P. J., and Nielsen, B. V.: Methane production from *Sargassum muticum*: effects of seasonality and of freshwater washes, *Energy and Built Environment*, 2, 235–242,   
700 <https://doi.org/10.1016/j.enbenv.2020.06.011>, 2021.

Marchal, E. and Picaut, J.: REPARTITION ET ABONDANCE EVALUEES PAR ECHOINTEGRATION DES POISSONS DU PLATEAU IVOIRO-GHANEEN EN RELATION AVEC LES UPWELLINGS LOCAUX., 1977.

Marsh, R., Addo, K. A., Jayson-Quashigah, P.-N., Oxenford, H. A., Maxam, A., Anderson, R., Skliris, N., Dash, J., and Tompkins, E. L.: Seasonal Predictions of Holopelagic Sargassum Across the Tropical Atlantic Accounting for Uncertainty in Drivers and Processes: The SARTRAC Ensemble Forecast System, *Front. Mar. Sci.*, 8, 722524,   
705 <https://doi.org/10.3389/fmars.2021.722524>, 2021.

Milledge, J. J. and Harvey, P. J.: Golden tides: problem or golden opportunity? The valorisation of Sargassum from beach inundations, *J. Mar. Sci. Eng.*, 4, <https://doi.org/10.3390/jmse4030060>, 2016.

Niermann, U.: Distribution of *Sargassum natans* and some of its epibionts in the Sargasso Sea, *Helgolander Meeresunters*, 40,   
710 343–353, 1986.

Ody, A., Thibaut, T., Berline, L., Changeux, T., André, J.-M., Chevalier, C., Blanfuné, A., Blanchot, J., Ruitton, S., Stiger-Pouvreau, V., Connan, S., Grelet, J., Aurelle, D., Guéné, M., Bataille, H., Bachelier, C., Guillemain, D., Schmidt, N., Fauvelle, V., Guasco, S., and Ménard, F.: From in situ to satellite observations of pelagic Sargassum distribution and aggregation in the Tropical North Atlantic Ocean, *PLoS ONE*, 14, <https://doi.org/10.1371/journal.pone.0222584>, 2019.

715 Oyesiku, O. O. and Egunyomi, A.: Identification and chemical studies of pelagic masses of *Sargassum natans* (Linnaeus) Gaillon and *S. fluitans* (Borgessen) Borgesen (brown algae), found offshore in Ondo State, Nigeria, *African Journal of Biotechnology*, 13, 1188–1193, <https://doi.org/10.5897/AJB2013.12335>, 2014.

Podlejski, W., Descloitres, J., Chevalier, C., Minghelli, A., Lett, C., and Berline, L.: Filtering out false Sargassum detections using context features, *Front. Mar. Sci.*, 9, 960939, <https://doi.org/10.3389/fmars.2022.960939>, 2022.

720 Putman, N. F., Goni, G. J., Gramer, L. J., Hu, C., Johns, E. M., Triñanes, J., and Wang, M.: Simulating transport pathways of pelagic Sargassum from the Equatorial Atlantic into the Caribbean Sea, *Progress in Oceanography*, 165, 205–214, <https://doi.org/10.1016/j.pocean.2018.06.009>, 2018.

Putman, N. F., Lumpkin, R., Olascoaga, M. J., Triñanes, J., and Goni, G. J.: Improving transport predictions of pelagic Sargassum, *Journal of Experimental Marine Biology and Ecology*, 529, 2020.

725 REEM-CI: Rapport sur l'état de l'environnement marin et côtier de la Côte d'Ivoire, 2021.

Robledo, D., Vázquez-Delfín, E., Freile-Pelegrín, Y., Vázquez-Elizondo, R. M., Qui-Minet, Z. N., and Salazar-Garibay, A.: Challenges and Opportunities in Relation to Sargassum Events Along the Caribbean Sea, *Front. Mar. Sci.*, 8, 699664, <https://doi.org/10.3389/fmars.2021.699664>, 2021.

730 Rodríguez-Martínez, R. E., Medina-Valmaseda, A. E., Blanchon, P., Monroy-Velázquez, L. V., Almazán-Becerril, A., Delgado-Pech, B., Vázquez-Yeomans, L., Francisco, V., and García-Rivas, M. C.: Faunal mortality associated with massive

beaching and decomposition of pelagic Sargassum, *Marine Pollution Bulletin*, 146, 201–205, <https://doi.org/10.1016/j.marpolbul.2019.06.015>, 2019.

735 Saba, A. O., Fakoya, K. A., Adet, L., Sule, H. A., Ojewole, A. E., and Osho-Abdulgafar, N. F.: Sargassum influxes in West Africa: Impacts, challenges, and prospects for sustainable management, *Harmful Algae*, 150, 102982, <https://doi.org/10.1016/j.hal.2025.102982>, 2025.

740 Sissini, M. N., Barros Barreto, M. B. B., Széchy, M. T. M., Lucena, M. B., Oliveira, M. C., Gower, J., Liu, G., Oliviera Bastos, E., Milstein, D., Gusmão, F., Martinelli-Filho, J. E., Alves-Lima, C., Colepicolo, P., Ameka, G., deGraft-Johnson, K. A. A., Gouvêa, L. P., Torrano-Silva, B., Jeremias Mello, T., Costa Lotufo, L. V., and Horta, P. A.: The floating Sargassum (Phaeophyceae) of the South Atlantic Ocean – likely scenarios, *Phycologia*, 56, 321–328, <https://doi.org/10.2216/16-92.1>, 2017.

Skliris, N., Marsh, R., Appeaning Addo, K., and Oxenford, H.: Physical drivers of pelagic sargassum bloom interannual variability in the Central West Atlantic over 2010–2020, *Ocean Dynamics*, 72, 383–404, <https://doi.org/10.1007/s10236-022-01511-1>, 2022.

745 Solarin, B. B., Bolaji, D. A., Fakayode, O. S., and Akinnigbagbe, R. O.: Impacts of an invasive seaweed *Sargassum hystrix* var. *fluitans* (Børgesen 1914) on the fisheries and other economic implications for the Nigerian coastal waters, *IOSR Journal of Agriculture and Veterinary Science*, 7, 1–6, <https://doi.org/10.9790/2380-07710106>, 2014.

Sowah, W. N. A., Jayson-Quashigah, P.-N., Atiglo, D. Y., and Addo, K. A.: Socio-economic Impact of Sargassum Influx Events on Artisanal Fishing in Ghana, <https://doi.org/10.21203/rs.3.rs-1861970/v1>, 9 August 2022a.

750 Sowah, W. N. A., Jayson-Quashigah, P.-N., Atiglo, D. Y., and Addo, K. A.: Socio-economic Impact of Sargassum Influx Events on Artisanal Fishing in Ghana, <https://doi.org/10.21203/rs.3.rs-1861970/v1>, 9 August 2022b.

Thompson, T. M., Young, B. R., and Baroutian, S.: Pelagic Sargassum for energy and fertiliser production in the Caribbean: A case study on Barbados, *Renewable and Sustainable Energy Reviews*, 118, 109564, <https://doi.org/10.1016/j.rser.2019.109564>, 2020.

755 Thouvenin-Masson, C., Boutin, J., Échevin, V., Lazar, A., and Vergely, J.-L.: Influence of river runoff and precipitation on the seasonal and interannual variability of sea surface salinity in the eastern North Tropical Atlantic, *Ocean Science*, 20, 1547–1566, <https://doi.org/10.5194/os-20-1547-2024>, 2024.

760 van Tussenbroek, B. I., Hernández-Arana, H. A., Rodríguez-Martínez, R. E., Espinoza-Avalos, J., Canizales-Flores, H. M., González-Godoy, C. E., Barba-Santos, M. G., Vega-Zepeda, A., and Collado-Vides, L.: Severe impacts of brown tides caused by *Sargassum* spp. on near-shore Caribbean seagrass communities, *Marine Pollution Bulletin*, 122, 272–281, <https://doi.org/10.1016/j.marpolbul.2017.06.057>, 2017.

Wang, M. and Hu, C.: Mapping and quantifying Sargassum distribution and coverage in the Central West Atlantic using MODIS observations, *Remote Sensing of Environment*, 183, 350–367, <https://doi.org/10.1016/j.rse.2016.04.019>, 2016.

Wang, M., Hu, C., Barnes, B. B., Mitchum, G., Lapointe, B., and Montoya, J. P.: The great Atlantic Sargassum belt, *Science*, 365, 83–87, <https://doi.org/DOI:10.1126/science.aaw7912>, 2019.

765 Witherington, B., Hiram, S., and Hardy, R.: Young sea turtles of the pelagic Sargassum-dominated drift community: habitat use, population density, and threats, *Mar Ecol Prog Ser*, 463, 1–22, <https://doi.org/10.3354/meps09970>, 2012.

<https://doi.org/10.5194/egusphere-2026-2727>

Preprint. Discussion started: 11 June 2026

© Author(s) 2026. CC BY 4.0 License.



Yaw Atiglo, D., Jayson-Quashigah, P.-N., Sowah, W., Tompkins, E. L., and Addo, K. A.: Misperception of drivers of risk alters willingness to adapt in the case of sargassum influxes in West Africa, *Global Environmental Change*, 84, 102779, <https://doi.org/10.1016/j.gloenvcha.2023.102779>, 2024.

770